Population substructure and signals of divergent adaptive selection despite admixture in the sponge *Dendrilla antarctica* from shallow waters surrounding the Antarctic Peninsula

Running head: Admixture & adaptation in an Antarctic sponge

Authors

Carlos Leiva[1,2*], Sergi Taboada[1,3], Nathan J. Kenny[1], David Combosch[4], Gonzalo Giribet[5], Thibaut Jombart[6], Ana Riesgo[1]

1 Department of Life Sciences, The Natural History Museum of London, Cromwell Road, London SW7 5BD, UK.

2 Department of Genetics, Microbiology and Statistics, Faculty of Biology, University of Barcelona, Avinguda Diagonal 643, 08028, Barcelona, Spain.

3 Department of Biology, Faculty of Science, Autonomous University of Madrid, Darwin Street, 2, 28049, Madrid, Spain.

4 Marine Laboratory, University of Guam, Mangilao, GU, USA.

5 Deparment of Organismic and Evolutionary Biology, Harvard University, 26 Oxford Street, 02138 Cambridge, USA.

6 Department of Infectious Disease Epidemiology, London School of Hygiene and Tropical Medicine, Keepel Street, London WC1E 7HT, UK.

*Corresponding author: cleivama@gmail.com

Abstract

Antarctic shallow-water invertebrates are exceptional candidates to study population genetics and evolution, because of their peculiar evolutionary history and adaptation to extreme habitats that expand and retreat with the ice sheets. Among them, sponges are one of the major components, yet population connectivity of none of their many Antarctic species has been studied. In order to investigate gene flow, local adaptation, and resilience to near-future changes caused by global warming, we sequenced 62 individuals of the sponge *Dendrilla antarctica* along the Western Antarctic Peninsula (WAP) and the South Shetlands (~ 900 km). We obtained information from 577 ddRADseq-derived SNPs, using RADseq techniques for the first time with shallow-water sponges. In contrast to other studies in sponges, our 389 neutral SNPs dataset showed high levels of gene flow, with a subtle substructure driven by the circulation system of the studied area. However, the 140 outlier SNPs under positive selection showed signals of population differentiation, separating the central-southern WAP from the Bransfield Strait area, indicating a divergent selection process in the study area despite panmixia. Fourteen of these outliers were annotated, being mostly involved in immune and stress responses. We suggest that the main selective pressure on *D. antarctica* might be the difference in the planktonic communities present in central-southern WAP compared to the Bransfield Strait area, ultimately depending on sea-ice control of phytoplankton blooms. Our study unveils an unexpectedly long distance larval dispersal exceptional in Porifera, broadening the use of genome-wide markers within non-model Antarctic organisms.

Keywords: adaptation, ddRADseq, mitochondrial genome, RNA-Seq, SNPs, South Shetland Islands

1 | INTRODUCTION

The gene flow and phylogeographic patterns of Southern Ocean shallow-water marine invertebrates in general, and sponges in particular, are interesting for a number of reasons. From an evolutionary history perspective, the Southern Ocean provides a unique scenario for studying the impact of drastic environmental shifts on the population dynamics of marine species, with repeated Pliocene–Pleistocene glacial cycles being the major factor in shaping the current diversity and distribution of the Antarctic fauna (Thatje, Hillenbrand, & Larter, 2005). The alternation of glacial and interglacial periods might have especially affected shallow-water benthic invertebrates, eliminating most of the available habitat during glacial maxima (Thatje et al., 2005; Rogers, 2007; Allcock & Strugnell, 2012). These dramatic environmental events left characteristic signatures throughout the genome of these shallow-water invertebrates, most of which have only been assessed using traditional mitochondrial [a fragment of the *cytochrome* c *oxidase subunit I* gene (*COI*)] and nuclear (*18S* and *28S rRNAs* genes) markers (*e.g.* Krabbe, Leese, et al., 2010; Janosik, Mahon, & Halanych, 2011; González-Wevar, David, & Pulin, 2011; González-Wevar, Saucède, et al., 2013). Although shallow-water sponges form massive reefs dominating an important fraction of the available hard substrate in Antarctica (Dayton, 1989), no study has yet addressed the population genetics and connectivity of any of the 397 described sponges from this continent (Downey, Griffiths, Linse, & Janussen, 2012; Riesgo, Taboada, & Avila, 2015). To our knowledge, the only study incorporating analyses of the genetic diversity of an Antarctic sponge was conducted on the deep-sea species *Stylocordyla chupachups* using microsatellites (Carella, Agell, & Uriz, 2018), but we did not consider it as a population genetics and connectivity study because the authors only focused on the sponge clonal reproduction at a very small

scale (less than 2 km).

The Antarctic Peninsula is currently one of the most rapidly warming regions of the planet (Vaughan, Marshall, et al., 2003). The mean atmospheric temperature rose nearly 3 ºC during the second half of the 20th century (King, 1994; King & Harangozo, 1998; Turner, Colwell, et al., 2005), with profound consequences for ice sheets and glaciers (Cook, Fox, Vaughan, & Ferrigno, 2005). Moreover, the summer temperature of the surface waters adjacent to the WAP increased by more than 1 ºC during the same period (Meredith & King, 2005), threatening shallow-water Antarctic species, which are less resilient to temperature increases than species elsewhere (Peck & Conway, 2000), and whose essential biological functions are extremely sensitive to temperature fluctuations (Peck, Webb, & Bailey, 2004). This aspect is especially concerning for sponges, as all of them are sessile organisms known to have lecithotrophic larvae (Maldonado, 2006), which would imply limited dispersal abilities and therefore higher vulnerability (Pascual et al. 2017). However, although in the Southern Ocean the reproductive life history stages appear to have little influence in structuring genetic patterns (Halanych & Mahon, 2018), sponge larvae from other latitudes are not usually able to disperse over large distances (Pérez-Portela & Riesgo, 2018), with some exceptions (see Maldonado, 2006). This limited dispersal capabilities generally result in highly structured and isolated populations (Pérez-Portela & Riesgo, 2018), with high levels of inbreeding and a consequently reduced resilience (Botsford, White, et al., 2009). Hence, to assess the degree of resilience that Antarctic sponges will have under future predicted habitat shifts (IPCC 5th Assessment Report, 2013), it is urgent to investigate their connectivity patterns and gene flow.

Population genetics, which delves into the distribution of genetic diversity within and between populations, depends essentially on the presence of genetic variability to work with. The mitochondrial genome (mitogenome, mtDNA) has been widely used for population genetic and phylogenetic analyses in Metazoa (Avise, Arnold, et al., 1987) due to its high substitution rates (Brown, George, & Wilson, 1979) and its maternal inheritance and haploidy (see Ernster & Schatz, 1981). However, in some early-splitting animal lineages, such as the members of the phylum Porifera, mtDNA variation within and between species is extremely low, due to its slow-evolving nature (Huang, Meier, Todd, & Chou, 2008a). With some notable exceptions (Duran & Rützler, 2006; DeBiasse, Richards, & Shivji, 2010; López-Legentil & Pawlik, 2009; Xavier, Rachello-Dolmen, et al., 2010), intraspecific relationships in sponges have therefore only been recently addressed using microsatellites (*e.g.* Calderón, Ortega, et al., 2007; Blanquer & Uriz, 2010; Giles, Saenz-Agudelo, et al., 2015; Riesgo, Pérez-Portela, et al., 2016; Taboada, Riesgo, et al., 2018). Within the past few years, new promising approaches for population genetics based on reduced representation genomic libraries combined with high-throughput sequencing techniques, like restriction-associated DNA sequencing (RADseq) and genotyping by sequencing (GBS), have become routinely implemented in marine invertebrates but hardly on early-splitting lineages (reviewed in Pérez-Portela & Riesgo, 2018). These methods are revolutionizing the ecological, evolutionary and conservation genetic fields because of their power to recover hundreds to thousands of neutral single nucleotide polymorphisms (SNPs) for fine-scale population analyses (Andrews, Good, et al., 2016). However, only one study to date recovered SNPs in sponges, which used amplicon sequencing to obtain 67 SNPs and detect the small-scale genetic structure of *Aphrocallistes vastus* (Brown, Davis, & Leys, 2017), the main reef-building glass sponge of

114 the British Columbia continental shelf.

115 To date, the analysis of RADseq-derived SNPs has just reached Antarctic marine
116 invertebrates with only four studies addressing the population genetic structure of the
117 Antarctic krill *Euphausia superba* (Deagle, Faux, et al., 2015), the brittle stars *Ophionotus*
118 *victoriae* (Galaska, Sands, et al., 2017a) and *Astrotoma agassizii* (Galaska, Sands, et al.,
119 2017b), and the sea spider *Nymphon australe* (Collins, Galaska, Halanych, & Mahon, 2018).
120 Although RADseq data can potentially be used for discovering genomic regions under
121 selective pressure (Catchen, Hohenlohe, et al., 2017; McKinney, Larson, Seeb, & Seeb,
122 2017), none of the above-mentioned studies has used this approach to delve into the footprints
123 that natural selection and local adaptation left in the genome of the three Antarctic species
124 listed above. In contrast, in other latitudes, RADseq has been successfully used to enable the
125 detection of loci under selection, providing the grounds to understand processes of adaptive
126 ecological divergence in a range of non-model marine organisms (*e.g.* Araneda, Larraín,
127 Hecht, & Narum, 2016; Ferchaud & Hansen, 2016; Gleason & Burton, 2016; Combosch,
128 Lemer, et al., 2017).

129 The dendroceratid *Dendrilla antarctica* Topsent, 1905 is one of the dominant sponges
130 inhabiting West Antarctic shallow waters (Sarà, Balduzzi, et al., 1992), playing a key role by
131 providing shelter and food for many other marine invertebrates (*e.g.* Moles, Wägele, et al.,
132 2017). Its distribution spans along the Antarctic Peninsula and its associated islands, to the
133 South Orkney Archipelago as the northernmost point of its species range (data from World
134 Porifera Database: www.marinespecies.org/porifera/porifera.php?p=taxdetails&id=164875).
135 *Dendrilla antarctica* is a brooding sponge, with yolky lecithotrophic larvae that are released

during the Antarctic summer (Koutsouveli, Taboada, et al., 2018). In the present study, we aim to assess the genetic diversity, demographic history, and genetic connectivity of *D. antarctica* at a regional scale in the Western Antarctic Peninsula (WAP) and South Shetland Islands using ddRADseq-derived SNPs (double digested RADseq). We also evaluate the suitability of the full mitochondrial genome in *D. antarctica* to assess genetic diversity and connectivity. Finally, we test for genetic signatures of divergent selection using SNPs identified in a F_{ST} outlier test, and measure the expression levels of the genes identified under selection in three transcriptome samples spanning the whole latitudinal range of our sampling area.

2 | MATERIALS AND METHODS

2.1 | Sample collection, preservation and DNA extraction

For the population genomics study with ddRADseq, we collected ~ 1 cm^3 of tissue from 67 specimens of *D. antarctica* during the 2015–2016 austral summer in seven locations across the WAP and the South Shetland Islands (Figure 1; Table 1). Sampling was performed by SCUBA diving at 5–25 m depth. Sponge fragments were preserved in 96% ethanol, the ethanol was replaced three times, and stored at -20 ºC until further processing. We extracted DNA from all samples using the DNeasy Blood & Tissue kit (Qiagen) following the manufacturer's protocol, with minor modifications in the cell lysis time (which was conducted with an overnight incubation) and the final DNA elution step (performed twice using 50 µL of elution buffer each time). DNA quantity was assessed with a Qubit dsDNA HS assay (Life Technologies).

For mitogenome reconstruction, we collected a fragment (~ 1 cm^3) of a specimen in 96% ethanol from Deception Island to perform draft-level genomic sequencing, with genomic DNA (gDNA) extracted as described above. Furthermore, we subsampled tissue fragments (~ 1 cm^3) of three individuals for additional mitogenome reconstruction and transcriptomic analysis, from three different sampling stations (O'Higgins Bay, n = 1; Deception Island, n = 1; and Adelaide Island, n = 1), covering the whole latitudinal range of the sponge in our study. We preserved the subsampled tissue fragments in RNA*later* (Life Technologies) immediately after collection, stored for 24h at 4 ºC, replaced the RNA*later* once, and then stored at -80 ºC until further processing.

2.2 | Transcriptomic and genomic library preparation and sequencing

For transcriptomics, total RNA was extracted using a standard trizol-based method using TRI Reagent (Life Sciences) following the manufacturer's instructions. Subsequent mRNA purification was performed with a Dynabeads mRNA Purification Kit (Invitrogen) also following the manufacturer's protocol. Three cDNA libraries were constructed with the ScriptSeq v2 kit (Illumina), using adapters 9, 10 and 11, and sequenced alongside other samples in a single flowcell of an Illumina NextSeq 500, at 150bp paired end read length at the sequencing unit of the NHM.

Our genomic library for mitogenome recovery was prepared using a TruSeq DNA PCR-free library kit (Illumina) and sequenced on an Illumina MiSeq at 150 bp nominal paired read length at the sequencing unit of the Natural History Museum, London (NHM).

2.3 | Transcriptome and mitochondrial assembly, and mitogenome screening

A total of 123,782,845 paired reads (Den_ROT_3 = 29,840,417 reads, Den_OH_2 = 39,434,819 reads, and Den_DEC_19 = 54,507,609 reads) were obtained in our transcriptomic run. A total of 9,644,983 paired raw reads were obtained in our gDNA run, 8,484,436 paired reads after trimming and filtering. Both transcriptomic and gDNA reads were cleaned using Trimmomatic 0.33 (Bolger, Lohse, & Usadel, 2014) with the following settings: ILLUMINACLIP:../Adapters.fa:2:30:10 LEADING:3 TRAILING:3 SLIDINGWINDOW:4:20 MINLEN:30 where the Adapters.fa file was substituted for the appropriate adapters for each library. Sequence quality was assessed before and after trimming using FastQC (Andrews, 2010) to ensure complete removal of adapter and low-quality sequence data. The final cleaned read files for transcriptomic analyses contained 26,523,504 reads for the sample Den_ROT_3, 30,645,339 reads for the sample Den_OH_2, and 49,611,670 reads for the sample Den_DEC_19.

Genomic DNA reads from the sample from Deception Island were assembled using Velvet 1.2.10 (Zerbino & Birney, 2008) at *k*-mer sizes of 71 and 91, which were the best *k*-mers after optimization trials. A local BLAST database was made from these gDNA assemblies using the makeblastdb command (Altschul, Madden, et al., 1997). The complete mitochondrial protein-coding sequence for the gDNA sample was obtained by blasting (tBLASTN) the complete mitochondrial genome of *Igernella notablis* (NC_010216) to these assemblies and extracting the best-hit contigs. Reciprocal BLASTX of the translated nucleotide sequences to the nr database confirmed the homology of these assemblies to Porifera, Dendroceratida.

The three individual transcriptomes were assembled into a *de novo* reference transcriptome using Trinity v 2013_08_14 (Grabherr, Haas, et al., 2011) with standard

205 settings except for a minimum contig length of 200 bp and *in silico* read normalization. This
206 *de novo* reference transcriptome contained 74,762 transcripts with an N50 of 658 and a total
207 of 38.8 Mb with GC content of 44.9%. Similarly, the three samples were assembled separately
208 using the same Trinity pipeline as above. In addition to the complete mitochondrial genome
209 recovered from the gDNA sample, three more mitochondrial genomes were obtained from the
210 transcriptomic reads or the assembled transcriptomes using the pipeline Trimitomics (Plese,
211 Rossi, et al., 2018). Subsequently, all four mitochondrial genomes (one coming from the
212 gDNA sample and three from the transcriptomes) were aligned in Geneious 8.1.8 (Kearse,
213 Moir, et al., 2012) using the Q-INS-I algorithm of MAFFT v7 (Katoh & Standley, 2013),
214 which is used as the default algorithm for rRNA alignments because it considers secondary
215 structure information, as a form of base-pairing probability (Katoh & Toh, 2008). The
216 software DNAsp 5.10.01 (Librado & Rozas, 2009) was used to calculate the number of
217 segregating sites (*S*), haplotype number (*H*), haplotype diversity (*H*d), and nucleotide
218 diversity (π).
219
220 **2.4 | ddRADseq library preparation and sequencing**
221 Library preparation was conducted following Peterson, Weber, et al. (2012) with the
222 following modifications (as in Combosch et al., 2017). Genomic DNA (100–1000 ng) was
223 digested using the high-fidelity restriction enzymes Sbf1 and EcoR1 (New England Biolabs).
224 Resulting digested fragments were cleaned with an Apollo 324 (IntegenX) using Agencourt
225 AMPure beads (1.5X volume ratio; Beckham Coulter), and were subsequently quantified with
226 a Qubit dsDNA HS assay (Life Technologies). Resulting fragments were ligated to custom-
227 made P1 and P2 adapters containing sample-specific barcodes and primer annealing sites.

228 Individually barcoded samples were pooled into libraries, cleaned by manual pipetting using
229 AMPure beads (1.5X volume ratio), and size-selected (270 to 600 bp) using a Pippin Prep
230 (Sage Science). Each library was then PCR-amplified using Phusion polymerase with 14–20
231 PCR cycles (98 ºC for 10 s, 65 ºC for 30 s and 72 ºC for 90 s, with an initial denaturation step
232 at 98 ºC for 30 s and a final extension step at 72 ºC for 5 min). Resulting libraries were
233 cleaned with an Apollo 324 to remove remaining adapters and primers using AMPure beads
234 (0.8X volume ratio). Each library was quantified using a qPCR Kapa library quantification kit
235 (Kapa Biosystems) and quality-checked on an Agilent BioAnalyzer 2100 (Agilent
236 Technologies). Libraries were pooled normalizing their concentration, subsequently pooled
237 with RNA-seq libraries in the same flowcell, and paired-end sequenced (150 bp) on an
238 Illumina HiSeq 2500 (Illumina) at the Center for Systems Biology, Harvard University
239 (Cambridge, MA, USA).
240
241 **2.5 | ddRADseq locus assembly and outlier detection**
242 Quality filtering and locus assembly was conducted with the Stacks pipeline, v 1.44 (Catchen,
243 Hohenlohe, et al., 2013). RAD-tags (DNA fragments with the two appropriate restriction
244 enzyme cut sites that were selected, amplified, and sequenced) were processed using
245 *process_radtags*, where raw reads were quality-trimmed to remove low quality reads, reads
246 with uncalled bases, and reads without a complete barcode or restriction cut site. The
247 *process_radtags* rescue feature (-r) was used to recover minimally diverged barcodes and
248 RAD-tags (--barcode_dist 3; --adapter_mm 2). The *process_radtags* trimming feature (-t) was
249 used to trim remaining reads to 120bp, in order to increase confidence in SNP calling. After
250 performing these filtering steps in *process_radtags*, we retained a total of 161,847,986 reads

from the initial 220,380,548 raw reads, with an average of 2,247,889 reads per sample. Preliminary tests were carried out following Jeffries, Copp, et al. (2016) to identify optimal Stacks parameters. Final parameter values were as follows: *ustacks*: M = 2, m = 3, allowing for gaps (--gapped; --max_gaps 3; --min_aln_len 0.80), using the removal (-r) and deleveraging (-d) algorithms; *cstacks*: n = 4, allowing for gaps (--gapped; --max_gaps 3; --min_aln_len 0.80); *sstacks*: allowing for gaps (--gapped). Mean locus coverage among all samples was 47,435, ranging from 23,359 to 199,138.

The Stacks *populations* module was used to conduct a first filtering of the data, retaining those SNPs present in at least 20% of the individuals (r = 0.2). To prevent the analysis of physically linked loci, and hence meet the assumptions of subsequent analyses, we used the "--write_single_SNP" option to retain only the first SNP from each RAD-tag. A subsequent more accurate filtering was performed using the *adegenet* R package (Jombart, 2008; Jombart & Ahmed, 2011; R Core Team, 2014), assessing SNP distributions across individual samples and sampling stations, and testing different filtering thresholds in order to maximize the number of retained SNPs and minimize missing data. This approach provides significant help in defining final thresholds in comparison with the Stacks *populations* module. Thus, we finally retained loci present in at least 40% of the individuals, and filtered out individuals with less than 30% of the final loci, resulting in a dataset containing 577 SNPs and 62 individuals.

In order to differentiate neutral SNPs from putative SNPs under positive selection, the database containing 577 SNPs was analyzed using default parameters in LOSITAN (Antao, Lopes, et al., 2008). We used LOSITAN because it implements the FDIST2 approach of Beaumont & Nichols (1996), which provides a robust method when populations deviate from

274 the island model of migration (Tigano, Shultz, et al., 2017). Also, it incorporates
275 heterozygosity and simulates a distribution for neutrally distributed markers (Narum & Hess,
276 2011; De Mita, Thuillet, et al., 2013). We considered that these features were more
277 appropriate for our model species studied herein, *Dendrilla antarctica*, than the characteristics
278 of other F_{ST}-outlier methods. Moreover, we also run Bayescan (Foll & Gaggioti, 2008) with
279 default parameters, which only detected one locus under selection already detected by
280 LOSITAN. We discuss LOSITAN results given the reasons stated above.
281
282 **2.6 | Population genetic analyses**
283 The neutral SNP dataset (389 SNPs, 62 organisms, vcf file in Supplementary Material 1) was
284 used for the population genetic analyses. Genetic diversity and demographic statistics were
285 calculated using *ape* (Paradis, Claude, & Strimmer, 2004), *pegas* (Paradis, 2010), and
286 *adegenet* R packages. The expected (*He*) and observed (*Ho*) heterozygosities per SNP were
287 extracted and subsequently averaged across samples within sampling stations from the
288 *adegenet* '*genind*' objects, and then the *hw.test* function in *pegas* was used to test for
289 deviations from Hardy-Weinberg equilibrium per SNP. To test whether *D. antarctica*
290 populations were in expansion we used the *tajima.test* function in *pegas* to obtain the
291 Tajima's *D* statistic for each sampling site and for the whole set of samples together. To
292 assess inbreeding within sampling stations and differentiation among them, we used F_{IS} and
293 F_{ST} *F*-statistics respectively, both obtained with the *fstat* function in the R package *hierfstat*
294 (Goudet, 2005).
295 Population structure was assessed using the function *snapclust* in the R package
296 *adegenet* (Beugin, Gayet, et al., 2018), the discriminant analysis of principal components

297 (DAPC) as implemented in the *adegenet* R package (Jombart, Devillard, & Balloux, 2010),
298 and STRUCTURE v 2.3 (Pritchard, Stephens, & Donnelly, 2000). STRUCTURE and
299 *snapclust* may produce similar individual membership probability plots, but they have totally
300 different approaches to the genetic clustering problem: while STRUCTURE uses a Bayesian
301 approach with Markov chain Monte Carlo (MCMC) to estimate allele frequencies in each
302 cluster and population memberships for every individual, *snapclust* is a fast likelihood
303 optimization method combining both model-based and geometric clustering approaches,
304 which uses the Expectation-Maximization (EM) algorithm to assign genotypes to populations
305 and detect admixture patterns. Initial group memberships for *snapclust* were chosen using the
306 k-means algorithm (pop.ini = "kmeans"), allowing a maximum *K* (number of clusters) of 10
307 (max = 10), and a maximum number of iterations of 100 (max.iter = 100). The analysis
308 successfully converged at the second iteration. The DAPC analysis was performed by
309 grouping samples by sampling stations, and the number of retained PCA axes was chosen
310 using the cross-validation *xvalDapc* function in the *adegenet* R package. STRUCTURE was
311 run twice, using two distinct datasets: (i) all neutral SNPs (389 SNPs, 62 individuals) and (ii)
312 just the neutral SNPs in Hardy-Weinberg equilibrium (210 SNPs, 62 individuals). Both
313 analyses were run for 200,000 MCMC iterations using the admixture model, with a burn-in of
314 100,000 iterations, setting the putative *K* (number of clusters) from 1 to 10 with 20 replicates
315 for each run. STRUCTURE HARVESTER (Earl & vonHoldt, 2012) and CLUMPP v 1.1.2
316 (Jakobsson & Rosenberg, 2007) were used to determine the most likely number of clusters
317 and to average each individual's membership coefficient across the *K* value replicates,
318 respectively.
319 Pairwise F_{ST} values were estimated to measure the differentiation between pairs of

sampling stations using the *pairwise.fst* function in the *hierfstat* R package. Their significance was tested with 1,000 permutations using the *ade4* R package (Dray & Dufour, 2007). The software Barrier v 2.2 (Manni, Guerard, & Heyer, 2004) was then used to identify and position genetic breaks in the sampling area. This software uses an improved Monmonier's algorithm to detect genetic barriers from a matrix of genetic distances (pairwise F_{ST} table) linked to a matrix of geographic distances. A Mantel test was performed to test the isolation by distance model, examining the correlation between geographic (accounting for coastlines) and genetic distances, using the *mantel.randtest* function in the *ade4* R package.

In order to test whether the DAPC grouping or the Barrier's genetic break explained a significant part of the total genetic variation, two hierarchical analyses of molecular variance (AMOVA) were performed using the *poppr.amova* function in the *poppr* R package.

Finally, in order to identify gene flow patterns in our study area, Nei's G_{ST} method was used to estimate the relative contemporary migration between sampling stations, using the *divMigrate* function of the *diveRsity* R package (Keenan, McGinnity, et al., 2013).

2.7 | Annotation, expression values, and structure of putative loci under selection

To improve the annotation step, all RAD-loci containing an outlier SNP under positive selection were mapped back to our *de novo* reference transcriptome using CLC Genomics Workbench 5.1 local blast (Altschul, et al., 1997) to obtain the contig for each RAD-locus. All contigs with uniquely mapped loci were then subjected to a BLASTX and BLASTN search against *nr* (default parameters, Altschul, et al., 1997), and this annotation was retained for the mapped RAD-locus. A functional annotation analysis was then performed using DAVID 6.8 (Huang, Sherman, & Lempicki, 2008b, 2008c). Expression values for putative contigs under

343 selection in each of the three RNA-Seq datasets were determined by mapping reads from
344 individual samples to the *de novo* reference transcriptome using the RSEM package (Li &
345 Dewey, 2011; --aln_method bowtie2) in Trinity (Grabherr, et al., 2011). The
346 abundance_estimates_to_matrix.pl script was used to determine comparable values of
347 expression (cross-sample normalization: Trimmed Mean of M-values, TMM), and the
348 obtained TMM values were subsequently normalised to TPM values (Transcripts Per
349 Kilobase Million).

350 In order to detect signals of geographically divergent adaptive selection, we used the
351 same structuring analyses used for the neutral SNP dataset. Hence, STRUCTURE, *snapclust*,
352 and DAPC were run for the dataset containing the SNPs under positive selection (140 SNPs,
353 62 individuals, vcf file in Supplementary Material 2) using the same parameters mentioned
354 above for the neutral dataset. Moreover, global F_{ST} statistic and pairwise F_{ST} values were
355 estimated using the *hierfstat* and *ade4* R packages as specified for the neutral dataset. The
356 software Barrier was also used on the loci under positive selection and, subsequently, two
357 AMOVA analyses were also performed in the *poppr* R package to test whether the DAPC
358 grouping or the Barrier's genetic break explained a significant part of the genetic variation.

359

360 **3 | RESULTS**

361

362 **3.1 | Mitogenome diversity**

363 The total length of the mitochondrial genome obtained from our gDNA reads from Deception
364 Island was 19,498 bp, of which 10,949 bp comprised protein-encoding sequences. From our
365 *de novo* transcriptomes, we were able to recover 10,859 bp for the sample from Adelaide

366 Island, 10,682 bp for the sample from Deception Island, and 10,893 bp for the sample from
367 O'Higgins Bay. The alignment of the four sequences encompassed 9,433 bp, with four
368 different haplotypes (*H*) but only three segregating sites (representing 0.032 % of the total)
369 (alignments of the 15 mitochondrial genes in Supplementary Material 3). Specifically, we
370 found one mutation in the gene ATP8 (site 141, T->A) in the transcriptomic sample from
371 Deception Island, one nucleotide varied in the sample from Adelaide Island in NAD4 (site
372 620, A->C), and finally one nucleotide varied in the gDNA sample from Deception Island in
373 the *cytochrome c oxidase I (COI)* gene (site 902, T->C). The nucleotide diversity (π) was
374 0.00016 ± 0.00004 and, since each of the four samples analyzed accounted for a different
375 haplotype, the haplotype diversity (*H*d) was 1.
376
377 **3.2 | Population genetics analyses using neutral SNPs**
378 Population genetics statistics are shown in Table 2. Tajima's *D* values were all negative,
379 showing significant *p*-values (*p*-value < 0.05) in all stations separately and for the whole
380 dataset (Table 2). Average expected heterozygosity (*H*e) ranged from 0.054 in Paradise Bay to
381 0.142 in King George Island, with a value of 0.162 when all samples were analyzed together
382 (Table 2). Average observed heterozygosity (*H*o) ranged from 0.052 in Paradise Bay to 0.079
383 in Half Moon Island, with a value of 0.067 for the whole dataset (Table 2). The number of
384 loci not found in Hardy-Weinberg equilibrium ranged from 0 in Paradise Bay to 27 in King
385 George Island, and a total of 178 loci when all samples were treated together (Table 2).
386 Inbreeding coefficient (F_{IS}) estimated from heterozygosity (F_{IS} = 1 - (*H*o/*H*e)) ranged from
387 0.037 in Paradise Bay to 0.616 in Adelaide Island, with a value of 0.586 for the entire dataset
388 (Table 2). *F*-statistics estimated in the *hierfstat* R package for all the samples together were

389 F_{IS} = 0.595, F_{ST} = 0.011.

390 The results of the STRUCTURE analysis for all neutral loci (389 SNPs) are shown in
391 Figure 2a. Although the most likely number of clusters was K = 4 [inferred from delta K
392 (Evanno, Regnaut, & Goudet, 2005), shown in Supplementary Material 4a] and many of the
393 samples were assigned to one of the 4 clusters with a high confidence, there is no clear pattern
394 of geographic structure from these results. In fact, STRUCTURE results may be interpreted as
395 an indication of panmixia or high gene flow among sampled stations. Similarly, *snapclust*
396 results (Figure 2b) revealed a lack of geographic structure, although the most likely number of
397 clusters for this analysis inferred from the AIC was K = 2 (see Supplementary Material 4b).
398 STRUCTURE results for the dataset just conaining the 210 SNPs in Hardy-Weinberg
399 equilibrium are shown in Supplementary Material 5. Due to the lack of geographic structure
400 in the results from both datasets, we retained information for all 389 SNPs in Figure 2a.

401 The two-dimensional representation of the DAPC results taking the first and second
402 DAPC axes showed differentiation of some of the sampling sites (Figure 2c), with O'Higgins
403 Bay and Adelaide Island appearing as the two most divergent stations (see Supplementary
404 Material 6a for the first-third DAPC axes representation, showing a similar population
405 structuring). Adelaide Island is the southernmost site in our sampling area, while O'Higgins
406 Bay represents the northernmost sampled area in the Antarctic Peninsula, which is in fact
407 oceanographically isolated by the Peninsula Front (see Figure 1b).

408 Pairwise F_{ST} comparisons showed low-to-moderate F_{ST} values ranging from 0 to 0.124
409 (Table 3, above diagonal). Although all F_{ST} values were non-significant, they allowed us to
410 identify genetic barriers in *D. antarctica*'s genetic landscape using the Barrier software. The
411 strongest genetic break separated O'Higgins Bay and King George Island stations from the

412 rest of the sampling localities (Figure 2d). The Mantel test indicated no correlation between
413 the geographic distance matrix and the genetic distance matrix (*p*-value = 0.687), refuting the
414 isolation by distance hypothesis and thus indicating that other factors (*e.g.* oceanographic
415 features) might be explaining the geographic distribution of *D. antarctica*'s genetic diversity.
416 The full migration G_{ST} table is shown in Supplementary Material 7. The highest
417 migration values (> 0.8) are represented in the migration network (Figure 3), indicating an
418 isolation of the Central Antarctic Peninsula (Cierva Cove and Paradise Bay), and high
419 contemporary migration between Adelaide Island and the South Shetlands, and within the
420 South Shetlands. High contemporary migration was also detected from O'Higgins Bay to
421 King George Island (Figure 3).
422 The AMOVA results for the neutral SNP dataset are shown in Table 4a. Both the
423 DAPC and the Barrier groupings appeared to be non-significant portions of the genetic
424 variance (p-values = 0.468 and 0.248, respectively), the two of them representing less than
425 1 % of the total variation (Table 4a).
426
427 **3.3 | Putative loci under selection**
428 A total of 188 F_{ST} outlier SNPs were detected by LOSITAN, 48 of them identified as
429 under balancing selection and 140 as under positive selection. These 140 SNPs represented
430 24.3 % of the complete SNPs dataset.
431 From the 140 RAD-tags with outlier SNPs under positive selection, 31 matched
432 contigs in our *de novo* assembled reference transcriptome of *Dendrilla antarctica* and for 16
433 of them we retrieved a blast hit against the *nr* NCBI database with evalue 1e-05 or lower
434 (Table 5). One of them corresponded to an uncharacterized protein, and another one matched

435 a bacterial aminotransferase (Table 5). This low ratio of only one RAD-tag matching a
436 bacterial gene out of the 140 under positive selection (0.7 %) is in agreement with previous
437 knowledge on the microbiome of *D. antarctica,* which is considered a low microbial
438 abundance sponge (Koutsouveli et al., 2018). For the 14 remaining annotated loci, gene
439 characterization and DAVID functional annotation analysis assigned them to six cellular
440 functions (Figure 4): (i) cytoskeleton reorganization, cell morphology, and motility, (ii)
441 ubiquitination, (iii) apoptosis, (iv) response to environmental stressors, (v) biological
442 detoxification, and (vi) RNA post-transcriptional modifications. The expression levels of
443 these genes were relatively similar across two of the sampling sites, Adelaide Is. and
444 O'Higgins Bay (Table 5), with almost all values within each gene in the same order of
445 magnitude, and nearly all genes overexpressed in the individual from Deception Island (Table
446 5; Figure 4). Only one gene appeared overexpressed in the individual from O'Higgins Bay
447 (*DNAH3*) and three genes overexpressed (*IPP*, *PLGR1*, and *PAE1850*) in the individual from
448 Adelaide Island (Table 5; Figure 4).

449 The results of the STRUCTURE analysis for the 140 SNPs under positive selection are
450 shown in Figure 5a. The most likely number of clusters was $K = 2$, with $K = 5$ as the second
451 most likely number of clusters (inferred from delta *K*, shown in Supplementary Material 4c).
452 These results indicate a lack of geographic structure in the dataset under positive selection,
453 which may be the result of the high migration and gene flow detected in the neutral dataset.
454 Similarly, *snapclust* (Figure 5b) did not retrieve any clear geographic structure for the 5
455 clusters inferred from AIC (see Supplementary Material 4d).

456 The representation of the DAPC results based on the 140 SNPs under positive
457 selection taking the first and second DAPC axes is shown in Figure 5c (See Supplementary

458 Material 6b for the first-third DAPC axes representation). Samples from the Bransfield Strait
459 stations (i.e. South Shetland Islands, O'Higgins Bay, and Cierva Cove) were grouped
460 together, while Paradise Bay and Adelaide Is. appeared as the most divergent sites (Figure
461 5c), the latter being the most differentiated sampling station based on the first eigenvalue.

462 F_{ST} statistic for the 140 SNPs under positive selection was estimated at 0.205 in the
463 *hierfstat* R package. Pairwise F_{ST} comparisons showed high and mostly significant F_{ST} values,
464 ranging from 0.017 to 0.421 (Table 3, below diagonal). The most robust genetic break
465 determined by the Barrier software using these pairwise F_{ST} values separated Cierva Cove
466 from the rest of the stations (Figure 5d).

467 AMOVA results for the under positive selection dataset are shown in Table 4b. The
468 Barrier grouping isolating Cierva Cove (Figure 5d) represented a non-significant 1.45 % of
469 the total variation (p-value = 0.124). On the other hand, the DAPC clustering separating
470 Adelaide Island, Paradise Bay, and the Bransfield Strait stations (Figure 5c) reached a
471 significant 6.72 % of the total genetic variance (p-value = 0.043).

472

473 **4 | DISCUSSION**

474

475 **4.1 | Mitogenome diversity**

476 Our study unveiled an extremely low mitochondrial diversity in *Dendrilla antarctica*, with
477 only four individual SNPs across 9,433 bp of protein-coding mitochondrial sequence data.
478 Although mitogenome sequences were only obtained from four individuals, the low
479 nucleotide diversity we observed in organisms spanning the whole latitudinal range of our
480 sampling area (ca. 900 km, which is almost the entire species distribution) indicates that

protein-coding mitochondrial markers provide almost no resolution for population genetic studies for *D. antarctica*. This extremely low variability in mitochondrial markers is not uncommon in sponges since *COI* has traditionally showed relatively low genetic variation at both intra- and interspecific levels (*e.g.* Dailianis, Tsigenopoulos, Dounas, & Voultsiadou, 2011; León-Pech, Cruz-Barraza, et al., 2015; Riesgo et al., 2016; Setiawan, Baldwin, Kaufmann, & Sturz, 2016; Taboada et al. 2018) with just a few exceptions (Duran & Rützler, 2006; DeBiasse et al., 2010; López-Legentil & Pawlik, 2009; Xavier et al., 2010), probably due to slower rates of mitochondrial genome evolution and/or the presence of active mitochondrial repair mechanisms (Huang et al., 2008a).

4.2 | Population genomic analyses using neutral SNPs

In contrast with the low variability of the mitochondrial genome in *D. antarctica*, our study revealed a high resolution power of ddRADseq-derived SNPs for population genetic studies. The analyses of our 389 neutral SNPs showed the characteristic signatures of a complex evolutionary history, likely the result of consecutive demographic shifts due to glacial cycles. For instance, significantly negative Tajima's *D* values were found in all sampling stations and in the whole dataset (Table 2), indicating a deviation in the haplotype frequencies from the neutrality model (Tajima, 1989). These results support the existence of a recent and rapid demographic expansion of *D. antarctica* in the WAP and the South Shetlands, which could have started after the last glacial–interglacial alternation (~ 20,000 – 10,000 years ago) when the last Antarctic shelf recolonization took place (see Allcock & Strugnell, 2012). This hypothesis has been suggested for other shallow-water Antarctic invertebrates (Thornhill, Mahon, Norenburg, & Halanych, 2008; Díaz, Féral, et al., 2011; González-Wevar et al., 2011;

504 Leiva, Riesgo, et al., 2018), which could have migrated northwards to sub-Antarctic islands
505 during glacial periods and recolonized the Antarctic shelf during interglacial periods. This
506 expansion–contraction model has already been tested for the Antarctic limpet *Nacella*
507 *concinna* (Strebel, 1908), demonstrating its glacial survival in the sub-Antarctic South
508 Georgia Island, followed by postglacial recolonization of the Antarctic Peninsula shelf
509 (González-Wevar et al., 2013).

510 Taking expected heterozygosity (*H*e) as a measure of the genetic diversity, as
511 originally defined (Nei, 1973), we found significantly lower genetic diversity values for *D.*
512 *antarctica* (Table 2: *H*e = 0.162 ranging from 0.054 to 0.142) than those reported for similar
513 population genetic studies on sponges using microsatellite markers (average *H*e ranging from
514 0.4 to 0.8; see Pérez-Portela & Riesgo, 2018), and lower than the *H*e values (from 0.24 to
515 0.323) reported in the only previously published study using SNPs in sponges (Brown et al.,
516 2017). In other examples using SNPs in different animal phyla, *H*e ranged from 0.298 to
517 0.312 in the salmon louse *Lepeophtheirus salmonis* (Jacobs, Noia, et al., 2018), from 0.211 to
518 0.214 in the Galapagos shark *Carcharhinus galapagensis* (Pazmiño, Maes, et al., 2017), or
519 from 0.128 to 0.276 in the sea anemone *Nematostella vectensis* (Reitzel, Herrera, et al., 2013),
520 thus corroborating our low values for *D. antarctica*. The extremely low genetic diversity of *D.*
521 *antarctica* could be related to the particular evolutionary history of the shallow-water
522 Antarctic benthic fauna, a consequence of the bottleneck events affecting benthic species
523 during glacial periods. These demographic events dramatically reduce genetic diversity after
524 population decimations, as has already been reported for other shallow-water Antarctic fauna
525 (see Allcock & Strugnell, 2012).

526 Our results revealed high admixture and lack of population differentiation, supported

527 by the low global F_{ST} of 0.011 and the non-significant pairwise F_{ST} values (Table 3),
528 suggesting high connectivity and dispersal capability of *D. antarctica* throughout the
529 sampling area, which covered most of the species distribution. We propose that this could be
530 due to the relatively long planktonic life of *D. antarctica* larvae, allowed by the great amount
531 of proteinaceous yolk that they contain (Koutsouveli et al*.,* 2018) in comparison with sponge
532 larvae from congeneric species from lower latitudes (*e.g.*, Ereskovsky & Tokina, 2004).
533 Furthermore, the strong oceanic currents in the study area (Zhou, Niiler, & Hu, 2002; Moffat,
534 Beardsley, Owens, & Van Lipzig, 2008; see Figure 1b) may increase the dispersal ability of
535 *D. antarctica* larvae. Remarkably, our results differ from most previous population genetic
536 studies on sponges, which generally report highly structured and differentiated populations,
537 even at local and regional scales (*e.g.* DeBiasse et al., 2010; Pérez-Portela et al., 2014; Riesgo
538 et al., 2016; Brown et al., 2017). Even compared to some oviparous sponges such as *Cliona*
539 *delitrix* which appears to disperse along the ~ 315 km of the Florida reef track (Chaves-
540 Fonnegra, Feldheim, Secord, & Lopez, 2015), our results suggested an unprecedent ~ 900 km
541 contemporary migration. However, although this long-distance connectivity is unusual in
542 sponges, it is common in Antarctic marine invertebrates. Examples of high gene flow are
543 shown in many Antarctic species, such as in the brittle stars *Astrotoma agassizii* (Galaska et
544 al., 2017a) and *Ophionotus victoriae* (Galaska et al., 2017b), the Antarctic limpet *Nacella*
545 *concinna* (González-Wevar et al., 2013), the nemertean *Parborlasia corrugatus* (Thornhill et
546 al., 2008), and the annelid *Pterocirrus giribeti* (Leiva et al., 2018).
547 In agreement with STRUCTURE and *snapclust* results, relatively high gene flow was
548 detected in our contemporary migration network between the South Shetlands and Adelaide
549 Island (Figure 3). We propose that these high migration values are a consequence of the

550 Antarctic Peninsula Coastal current (APCC) running southwards off the WAP (Moffat et al.,
551 2008; Figure 1b) and the ACC running northwards, connecting stations ca. 900 km. Other
552 high migration values were found within the South Shetlands Archipelago, and from
553 O'Higgins Bay to King George Island (Figure 3). This result could be explained by different
554 factors that may be occasionally weakening the Peninsula Front, an oceanic front produced by
555 the intrusion of a tongue of water from the Weddell Sea in the Bransfield Strait (Sangrà,
556 Gordo, et al., 2011; Figure 1b). For instance, its seasonality is not completely understood yet,
557 due to the sampling season solely extending during austral summer (Zhou, Niiler, Zhu, &
558 Dorland, 2006; Sangrà et al., 2011; Huneke, Huhn, & Schröeder, 2016). Also, the inter-frontal
559 anticyclonic eddy system found between the Peninsula Front and the Bransfield Current
560 (Sangrà et al., 2011) could be potentially interfering with the impermeability of the Peninsula
561 Front. Moreover, the Southern Annular Mode (SAM) and El Niño Southern Oscillation
562 (ENSO) have been found to play a role on the water masses distribution of the Bransfield
563 Strait (Dotto, Kerr, Mata, & Garcia, 2016; Barlett, Tosonotto, et al., 2018, respectively),
564 which may cause inter-annual variation of the Peninsula Front. Interestingly, our
565 contemporary migration network also showed that the most disconnected region in our study
566 area was the centre of the WAP, where both Cierva Cove and Paradise Bay sampling sites are
567 located (Figure 3). The oceanic features of our study area could also be behind the isolation of
568 this region, which is disconnected from other areas by the Peninsula Front in the north and by
569 the APCC in the west, running through the western side of the Palmer Archipelago (Moffat et
570 al., 2008; Figure 1b).
571 Despite the lack of strong population structure, DAPC detected slight patterns of
572 population differentiation between O'Higgins Bay, Adelaide Island, and the rest of sampling

573 stations. This differentiation could be driven by the contemporary oceanographic features in
574 the study area, with Adelaide Island as the southernmost sampling site and O'Higgins Bay
575 representing the area at the tip of the WAP isolated by the Peninsula Front. Accordingly, the
576 main genetic break we detected partially coincided with the Peninsula Front, but grouping
577 King George Island together with O'Higgins Bay (Figure 2d), which is in agreement with the
578 high migration flow from O'Higgins Bay to King George Island discussed above. A similar
579 genetic break coincident with the Peninsula Front has already been identified for the brittle
580 star *Ophionotus victoriae* using SNPs (Galaska et al., 2017a), and also for the intertidal
581 phyllodocid *Pterocirrus giribeti* using a fragment of the mitochondrial *COI* marker (Leiva et
582 al., 2018). In addition, different reproductive timing due to, for instance, the effects of north-
583 south differences in sea-ice retreat (Stammerjohn, Martinson, Smith, & Iannuzzi, 2008) could
584 also play a role in population substructure with distinct breeding groups (Sugg, Chesser,
585 Dobson, & Hoogland, 1996).

586 However, both DAPC and Barrier groupings appeared as a non-significant part of the
587 total genetic variation in the AMOVA analyses (Table 4a). This may be due to the high
588 admixture and migration detected in the neutral dataset (Figure 2a–2b; Figure 3), and hence
589 we suggest that both groupings should be understood as permeable barriers.

590

591 **4.3 | Signals of divergent adaptive selection**

592 In our SNP dataset we identified 140 outlier SNPs as candidates for positive selection. Based
593 on this dataset, we recovered a high F_{ST}-statistic value of 0.205, along with high and
594 significant pairwise F_{ST} values (Table 3, below diagonal), revealing geographically divergent
595 adaptive selection. In species with high levels of population connectivity, like *D. antarctica*

here, local adaptation requires high levels of divergent selection. This has already been reported for other marine invertebrates with planktonic larvae, such as the marine snail *Chlorostoma funebralis* (Gleason & Burton, 2016) and the red abalone *Haliotis rufescens* (De Wit & Palumbi, 2013), both from the Pacific coast of California in the USA. Other examples from fishes with a similar pattern are the Atlantic cod *Gadus morhua* (Barth, Berg, et al., 2017), and the Atlantic herring *Clupea harengus* (Limborg, Helyar, et al., 2012). These results are particularly relevant for the Southern Ocean, since they challenge the classic consideration of Antarctic organisms as stable and homogeneous along their distributions.

The STRUCTURE and *snapclust* results from the 140 SNPs under positive selection also showed the effects of the admixture and high migration discussed above in the neutral dataset (Figure 5a-b). However, we observed two unique genetic clusters at the central and southern WAP (Paradise Bay and Adelaide Island), one of them appearing at both stations (purple individuals at Figure 5b) and the other one exclusively present at Adelaide Island (blue individuals at Figure 5b). In agreement, the DAPC analysis clustered together all the stations from the Bransfield Strait area, separating Adelaide Island (as the most divergent sampling station) and Paradise Bay (Figure 5c). The significant 6.72 % of the variance explained by this DAPC grouping (Table 4b) suggests different selective pressures in the central-southern WAP (Adelaide Island and Paradise Bay) and in the Bransfield Strait area (remaining sampling stations).

In this scenario with divergent selective pressures promoting local adaptation, we identified the function of the genes with signatures of selection, with some of them related to the organization of the cytoskeleton (Figure 4). Two of these genes, *dynein heavy chain 3* (*DNAH3*) and *cilia and flagella associated protein 54* (*CFAP54*), are involved in the

619 assembly, function, motility and power stroke of flagella and cilia (Asai & Koonce, 2001;
620 Carter, 2013; McKenzie, Craige, et al., 2015). As most other sponges, *Dendrilla antarctica* is
621 a filter-feeding sponge that relies on the flagellar beating to modulate the inflow current for
622 particle feeding, and therefore we suggest that the selection signatures in the previously
623 mentioned genes might be related to divergent filtering abilities between the Bransfield Strait
624 area and the central and southern WAP. Furthermore, in general terms, cytoskeletal elements
625 are involved in the regulation of many cellular functions related to immune response, such as
626 cell migration, antigen recognition, and phagocytosis (Vicente-Manzanares & Sánchez-
627 Madrid, 2004). The gene *actin-binding protein IPP-like* (*IPP*) plays a role in organizing the
628 actin cytoskeleton (Ciobanasu, Faivre, & Le Clainche, 2013), which is essential for immune
629 responses (Wickramarachchi, Theofilopoulos, & Kono, 2010). In addition, heavy chain
630 dyneins such as *DNAH3* have also been reported to aid in the stress granules (SGs) formation
631 (Kwon, Zhang, & Matthias, 2007; Loschi, Leishman, Berardone, & Boccaccio, 2009). SGs
632 are cytosolic aggregations comprised of RNAs and RNA-binding proteins which appear in
633 response to different stressors, with important function in preserving mRNA and regulating its
634 translation during stress responses (Kedersha & Anderson, 2002). In addition, SGs also
635 prevent apoptosis (*e.g.* Buchan & Parker, 2009), contain antioxidant machinery (Takahashi,
636 Higuchi, et al., 2013), and are involved in cellular recovery after stress exposure (Kedersha,
637 Chen, et al., 2002). Gleason & Burton (2016) found a *heavy chain dynein* under positive
638 selection in the marine snail *Chlorostoma funebralis,* relating the selective pressure in this
639 locus to SGs formation and their function during thermal stress.

640 Furthermore, four other genes with functions related to apoptosis appeared under
641 positive selection throughout our sampling area (Figure 4). Apoptosis is a conserved

642 mechanism that occurs during antibacterial response in sponges (Wiens, Korzhev, et al.,
643 2007). Da Fonseca, Kosiol, et al. (2010) reviewed previous studies on selective pressure in
644 apoptosis-related genes, concluding that positive selection in apoptotic genes is caused by
645 their immune function. Indeed, some of the other genes under positive selection in our dataset
646 were related to ubiquitination (Figure 4), a function also related to the immune system, as it
647 regulates the pattern-recognition receptor signaling that mediates immune responses (Hu &
648 Sun, 2016). Moreover, ubiquitination has been related to local adaptation in corals, where it
649 responds to different environmental factors that cause stress (Bay & Palumbi, 2014; Jin,
650 Lundgren, et al., 2016; van Oppen, Bongaerts, et al., 2018). This is due to its role in removing
651 macromolecular debris such as reactive oxygen species (ROS) generated by cellular stress
652 (Kültz, 2003). Interestingly, *dimethylaniline monooxigenase 5* (*FMO5*), the enzyme resulting
653 from one of the genes under positive selection retrieved here for *D. antarctica*, catalyses the
654 oxygenation of N,N-dimethylanilines, a reaction present in the ROS biological detoxification
655 pathway (Jakoby, Bend, & Caldwell, 2012). Furthermore, *CD163*, which also appeared to be
656 under positive selection here, is associated with the immune system and the response to
657 environmental stressors as well (Figure 4; Fabriek, van Bruggen, et al., 2009; Burkard,
658 Lillico, et al., 2017). Finally, two RNA post-transcriptional modification genes were identified
659 as under positive selection (Figure 4). This mechanism aids gene regulation under various
660 cellular stress situations (*e.g.* Anderson & Kedersha, 2009; Chinnusamy, Zhu, & Zhu, 2007;
661 Filipowicz, Bhattacharyya, & Sonenberg, 2008; Floris, Mahgoub, et al., 2009).
662 The signatures of selection in stress and immune responses that we detected are mostly
663 related to the molecular toolkit that sponges, which are generally filter-feeders, use to
664 discriminate between, and react to, food, pathogens and symbionts in the seawater that they

665 filter and runs through their bodies (Pita, Hoeppner, Ribes, & Hentschel, 2018). Hence,
666 different microbiome complements in the seawater in different areas would elicit divergent
667 adaptive strategies in sponges in the particular genes that we detected here as under positive
668 selection. Interestingly, differences in sea-ice duration in the Antarctic Peninsula's shallow
669 waters usually translate into highly divergent seawater microbiota, both in composition and
670 abundance (Vernet, Martinson, et al., 2008; Ducklow, Fraser, et al., 2012). While total sea-ice
671 duration in the vicinity of Adelaide Island is around 250 days a year, with a summer sea-ice
672 retreat, total sea-ice duration is below 150 days in the other sampling stations, generally with
673 spring retreats (Stammerjohn, Martinson, Smith, & Iannuzzi, 2008). This difference in sea-ice
674 duration is key to maintaining vastly different planktonic communities between southern
675 WAP and the Bransfield Strait area, because the presence and magnitude of phytoplankton
676 blooms in the Southern Ocean are regulated by the timing of sea-ice retreat (Vernet et al.,
677 2008; Ducklow et al., 2012; Luria, Ducklow, & Amaral-Zettler, 2014). Generally, the later the
678 sea-ice retreats, the higher the phytoplankton productivity, as a consequence of sea-ice
679 inhibition of the formation of a spring deep mixed layer, which in turn inhibits phytoplankton
680 (Ducklow et al., 2012). Furthermore, phytoplankton–bacteria trophic coupling has been
681 demonstrated in the Antarctic Peninsula by the direct bacterial assimilation of recent
682 photosynthetic products (Morán, Gasol, Pedrós-Alió, & Estrada, 2001; Morán & Estrada,
683 2002) and by the bacterial dependence on DOM, which in turn depends on phytoplankton
684 (Ducklow et al., 2012). Apart from the effects on the planktonic communities, a later sea-ice
685 retreat produces fresher and colder summer surface waters in the southern WAP, due to more
686 recent or ongoing seasonal ice melting (Ducklow et al., 2012).
687 Thus, due to the ice–plankton interaction outlined above, phytoplankton and bacterial

688 communities, as well as summer surface water temperature, widely differ between the
689 southern WAP, and the Bransfield Strait area. Since sponges are able to feed on both diatoms
690 and bacteria, the different composition of these communities across our study area could
691 potentially drive local adaptation of *D. antarctica* populations, not only because of their
692 relevant role in food availability, but also as potential agents of diseases and other stresses.
693 Further studies will be directed to test whether this local adaptation hypothesis we suggest for
694 *D. antarctica* is a general pattern also present in other benthic filter-feeding invertebrates
695 sampled in the same studied area, or even whether micro-plankton composition generally
696 drives adaptation of sponges.

697 A comparison of normalized expression values for the 14 annotated genes under
698 positive selection showed that most of the variation occurred between the sample from
699 Deception Island and the other two samples (Table 5; Figure 4). This contrasts with the DAPC
700 results of the neutral and under positive selection datasets (Figures 2c and 5c), and it is
701 probably because of the physicochemical particularities of Deception Island waters, which is
702 an active volcano with a submerged caldera (Port Foster) where our samples were collected.
703 The waters of Port Foster are characterized by the presence of suspended volcaniclastic
704 particles (Baldwin & Smith, 2003) and chemicals from local geothermal activity (Elderfield,
705 1972; Deheyn, Gendreau, Baldwin, & Latz, 2005). Moreover, the fumarolic emissions and
706 geothermal springs spotting the sedimentary seafloor confer upon Port Foster unusually high
707 bottom-water temperatures of 2–3 ºC (Ortiz, Vila, et al., 1992). These features undoubtedly
708 affect and stress benthic filter feeders such as *D. antarctica*, and may have contributed to the
709 upregulation of genes related to different stresses. Proper differential gene expression analyses
710 will be conducted to test whether particular physicochemical water features at Deception

711 Island are determinant at shaping gene expression in a wide array of shallow-water
712 invertebrates, thus testing their adaptation potential at the transcriptome level.
713
714 **5 | CONCLUSIONS**
715 Overall, the current gene flow scenario for *D. antarctica* is characterized by high migration
716 and low population differentiation, with a subtle population substructure driven by the oceanic
717 features of the region. Remarkably, despite this background of population admixture, we
718 identified divergent selective pressures along the studied region that could be explained by the
719 sea-ice–benthos coupling via planktonic communities. Local adaptation was long assumed to
720 be erased when high population connectivity was present in marine organisms. But recent
721 investigations indicate that even though few larvae might suffice to maintain genetic
722 homogeneity between populations, that is hardly possible for loci under selection (Sanford
723 and Kelly, 2011). The implications of our results are therefore vast. Our relatively slight
724 patterns of local adaptation are indicative of the potential for plastic physiological responses
725 to environmental shifts. In addition, and in contrast to previous studies of shallow-water
726 sponges, we report a well-connected network of populations across approximately 1,000 km.
727 Our study therefore corroborates that populations that appear homogeneous for neutral loci, in
728 fact exhibit local adaptation. In this sense, our study suggests a finely tuned physiological
729 response to current conditions but high resilience to future changes for *D. antarctica* in the
730 Antarctic Peninsula. However, due to larval reliance on oceanic currents to maintain high
731 dispersal abilities, this exceptional gene flow might be threatened by changes that increasing
732 sea temperature could create in Southern Ocean oceanographic circulation patterns, which are
733 not completely understood yet (Meijers, 2014). Moreover, a general reduction of planktonic

734 larval duration is expected for all larvae in the near future, because their metabolic,
735 developmental, and growth rates are determined by water temperature (O'Connor, Bruno, et
736 al., 2007). Thus, a shorter larval stage could imply a reduction of the dispersal capabilities of
737 *D. antarctica*, with implications for its gene flow and resilience, due to a putatively higher
738 proportion of larvae dying before reaching a suitable settlement site, as has been proposed for
739 fish larvae (O'Connor et al., 2007; Kendall, Poti, et al., 2013). Therefore, our results can be
740 used as a baseline for future assessments of the effects of a changing Southern Ocean on the
741 population connectivity and resilience of *D. antarctica.*
742
743 **ACKNOWLEDGEMENTS**
744 We are indebted to Patricia Álvarez-Campos, Oriol Sacristán, Javier Cristobo, Juan Junoy,
745 Juan Moles, Carlos Angulo-Preckler, Blanca Figuerola, and Conxita Avila for their help
746 during sampling collection, and the Spanish Base 'Gabriel de Castilla' and 'BIO/Hésperides'
747 crew for their logistical support. We also thank the Giribet Lab for all the help and support
748 provided during library construction in the laboratory. Special thanks are given to Eugènia
749 Almacellas for her support during manuscript writing and for her brilliant suggestions and
750 ideas. We also thank four anonymous reviewers and the Editor for their valuable comments
751 and suggestions. This work was supported by two DIF grants of The Natural History
752 Museum, London (SDF14032 and SDR17012) to A.R., a Marie Sklodowska Curie grant
753 (IF750937) to N.J.K., and a grant of the Spanish Ministry of Economy and Competitiveness in
754 which A.R., S. T., G. G., and C. L. have been involved (DISTANTCOM: CTM2013-
755 42667/ANT).

REFERENCES

Ajuh, P., Sleeman, J., Chusainow, J., & Lamond, A. I. (2001). A direct interaction between the carboxyl terminal region of CDC5L and the WD40domain of PLRG1 is essential for pre-mRNA splicing. *Journal of Biological Chemistry, 276*, 42370–42381.

Allcock, A. L., & Strugnell, J. M. (2012). Southern Ocean diversity: new paradigms from molecular ecology. *Trends in Ecology & Evolution, 27*, 520-528.

Altschul, S. F., Madden, T. L., Schäffer, A. A., Zhang, J., Zhang, Z., Miller, W., & Lipman, D. J. (1997). Gapped BLAST and PSI-BLAST: a new generation of protein database search programs. *Nucleic Acids Research, 25*, 3389-3402.

Anderson, P., & Kedersha, N. (2009). RNA granules: post-transcriptional and epigenetic modulators of gene expression. *Nature Reviews Molecular Cell Biology, 10*, 430-436.

Andrews, K. R., Good, J. M., Miller, M. R., Luikart, G., & Hohenlohe, P. A. (2016). Harnessing the power of RADseq for ecological and evolutionary genomics. *Nature Reviews Genetics, 17*, 81.

Andrews, S. (2010) FastQC: A quality control tool for high throughput sequence data. Available online at: http://www.bioinformatics.babraham.ac.uk/projects/fastqc

Antao, T., Lopes, A., Lopes, R. J., Beja-Pereira, A., & Luikart, G. (2008). LOSITAN: a workbench to detect molecular adaptation based on a F_{ST}-outlier method. *BMC Bioinformatics, 9*, 323.

Araneda, C., Larraín, M. A., Hecht, B., & Narum, S. (2016). Adaptive genetic variation distinguishes Chilean blue mussels (*Mytilus chilensis*) from different marine environments. *Ecology and Evolution, 6*, 3632-3644.

Asai, D. J., & Koonce, M. P. (2001). The dynein heavy chain: structure, mechanics and evolution. *Trends in Cell Biology, 11*, 196-202.

Avise, J. C., Arnold, J., Ball, R. M., Bermingham, E., Lamb, T., Neigel, J. E., ... & Saunders, N. C. (1987). Intraspecific phylogeography: the mitochondrial DNA bridge between population genetics and systematics. *Annual Review of Ecology and Systematics, 18*, 489-522.

Baldwin, R. J., & Smith Jr, K. L. (2003). Temporal dynamics of particulate matter fluxes and sediment community response in Port Foster, Deception Island, Antarctica. *Deep Sea Research Part II: Topical Studies in Oceanography, 50*, 1707-1725.

Barlett, E. M. R., Tosonotto, G. V., Piola, A. R., Sierra, M. E., & Mata, M. M. (2018). On the temporal variability of intermediate and deep waters in the Western Basin of the Bransfield Strait. *Deep Sea Research Part II: Topical Studies in Oceanography, 149*, 31-46.

Barth, J. M., Berg, P. R., Jonsson, P. R., Bonanomi, S., Corell, H., Hemmer□Hansen, J., ... & Moksnes, P. O. (2017). Genome architecture enables local adaptation of Atlantic cod despite high connectivity. *Molecular Ecology, 26*, 4452-4466.

Bay, R. A., & Palumbi, S. R. (2014). Multilocus adaptation associated with heat resistance in reef-building corals. *Current Biology, 24*, 2952-2956.

Beaumont, M. A., & Nichols, R. A. (1996). Evaluating loci for use in the genetic analysis of population structure. *Proceedings of the Royal Society London B: Biological Sciences, 263*, 1619-1626.

Beugin, M. P., Gayet, T., Pontier, D., Devillard, S., & Jombart, T. (2018). A fast likelihood solution to the genetic clustering problem. *Methods in Ecology and Evolution, 9*, 1006-1016.

Blanquer, A., & Uriz, M. J. (2010). Population genetics at three spatial scales of a rare sponge living in fragmented habitats. *BMC Evolutionary Biology, 10*, 13.

Bolger, A. M., Lohse, M., & Usadel, B. (2014). Trimmomatic: a flexible trimmer for Illumina sequence data. *Bioinformatics, 30*, 2114-2120.

Botsford, L. W., White, J. W., Coffroth, M. A., Paris, C. B., Planes, S., Shearer, T. L., ... & Jones, G. P. (2009). Connectivity and resilience of coral reef metapopulations in marine protected areas: matching empirical efforts to predictive needs. *Coral Reefs, 28*, 327-337.

Brown, W. M., George, M., & Wilson, A. C. (1979). Rapid evolution of animal mitochondrial DNA. *Proceedings of the National Academy of Sciences of the USA, 76*, 1967-1971.

Brown, R. R., Davis, C. S., & Leys, S. P. (2017). Clones or clans: the genetic structure of a deep□sea sponge, *Aphrocallistes vastus*, in unique sponge reefs of British Columbia, Canada. *Molecular Ecology, 26*, 1045-1059.

Buchan, J. R., & Parker, R. (2009). Eukaryotic stress granules: the ins and outs of translation. *Molecular Cell, 36*, 932-941.

Burkard, C., Lillico, S. G., Reid, E., Jackson, B., Mileham, A. J., Ait-Ali, T., ... & Archibald, A. L. (2017). Precision engineering for PRRSV resistance in pigs: macrophages from genome edited pigs lacking CD163 SRCR5 domain are fully resistant to both PRRSV genotypes while maintaining biological function. *PLoS Pathogens, 13*, e1006206.

Calderón, I., Ortega, N., Duran, S., Becerro, M., Pascual, M., & Turon, X. (2007). Finding the relevant scale: clonality and genetic structure in a marine invertebrate (*Crambe crambe*, Porifera). *Molecular Ecology, 16*, 1799-1810.

Carella, M., Agell, G., & Uriz, M. J. (2018). Asexual reproduction and heterozygote selection in an Antarctic demosponge (*Stylocordyla chupachus*, Suberitida). *Polar Biology*, 1-9.

Carter, A. P. (2013). Crystal clear insights into how the dynein motor moves. *Journal of Cell Science, 126*, 705-713, jcs-120725.

Catchen, J. M., Hohenlohe, P. A., Bassham, S., Amores, A., & Cresko, W. A. (2013). Stacks: an analysis tool set for population genomics. *Molecular Ecology, 22*, 3124-3140.

Catchen, J. M., Hohenlohe, P. A., Bernatchez, L., Funk, W. C., Andrews, K. R., & Allendorf, F. W. (2017). Unbroken: RADseq remains a powerful tool for understanding the genetics of adaptation in natural populations. *Molecular Ecology Resources, 17*, 362-365.

Chaves-Fonnegra, A., Feldheim, K. A., Secord, J., & Lopez, J. V. (2015). Population structure and dispersal of the coral excavating sponge *Cliona delitrix*. *Molecular Ecology, 24*, 1447-1466.

Chinnusamy, V., Zhu, J., & Zhu, J. K. (2007). Cold stress regulation of gene expression in plants. *Trends in Plant Science, 12*, 444-451.

Ciobanasu, C., Faivre, B., & Le Clainche, C. (2013). Integrating actin dynamics, mechanotransduction and integrin activation: the multiple functions of actin binding proteins in focal adhesions. *European Journal of Cell Biology, 92*, 339-348.

Collins, E. E., Galaska, M. P., Halanych, K. M., & Mahon, A. R. (2018). Population genomics of *Nymphon australe* Hodgson, 1902 (Pycnogonida, Nymphonidae) in the Western Antarctic. *The Biological Bulletin, 234*, 190-191.

Combosch, D. J., Lemer, S., Ward, P. D., Landman, N. H., & Giribet, G. (2017). Genomic signatures of evolution in Nautilus—An endangered living fossil. *Molecular Ecology, 26*, 5923-5938.

Cook, A. J., Fox, A. J., Vaughan, D. G., & Ferrigno, J. G. (2005). Retreating glacier fronts on the Antarctic Peninsula over the past half-century. *Science, 308*, 541-544.

Da Fonseca, R. R., Kosiol, C., Vinař, T., Siepel, A., & Nielsen, R. (2010). Positive selection on apoptosis related genes. *Febs Letters, 584*, 469-476.

Dailianis, T., Tsigenopoulos, C. S., Dounas, C., & Voultsiadou, E. (2011). Genetic diversity of the imperilled bath sponge *Spongia officinalis* Linnaeus, 1759 across the Mediterranean Sea: patterns of population differentiation and implications for taxonomy and conservation. *Molecular Ecology, 20*, 3757-3772.

Dayton, P. K. (1989). Interdecadal variation in an Antarctic sponge and its predators from oceanographic climate shifts. *Science, 245*, 1484-1486.

Deagle, B. E., Faux, C., Kawaguchi, S., Meyer, B., & Jarman, S. N. (2015). Antarctic krill population genomics: apparent panmixia, but genome complexity and large population size muddy the water. *Molecular Ecology, 24*, 4943-4959.

DeBiasse, M. B., Richards, V. P., & Shivji, M. S. (2010). Genetic assessment of connectivity in the common reef sponge, *Callyspongia vaginalis* (Demospongiae: Haplosclerida) reveals high population structure along the Florida reef tract. *Coral Reefs, 29*, 47-55.

De Mita, S., Thuillet, A. C., Gay, L., Ahmadi, N., Manel, S., Ronfort, J., & Vigouroux, Y. (2013). Detecting selection along environmental gradients: analysis of eight methods and their effectiveness for outbreeding and selfing populations. *Molecular Ecology, 22*, 1383-1399.

De Wit, P., & Palumbi, S. R. (2013). Transcriptome□wide polymorphisms of red abalone (*Haliotis rufescens*) reveal patterns of gene flow and local adaptation. *Molecular Ecology, 22*, 2884-2897.

Deheyn, D. D., Gendreau, P., Baldwin, R. J., & Latz, M. I. (2005). Evidence for enhanced bioavailability of trace elements in the marine ecosystem of Deception Island, a volcano in Antarctica. *Marine Environmental Research, 60*, 1-33.

Díaz, A., Féral, J. P., David, B., Saucède, T., & Poulin, E. (2011). Evolutionary pathways among shallow and deep-sea echinoids of the genus *Sterechinus* in the Southern Ocean. *Deep Sea Research Part II: Topical Studies in Oceanography, 58*, 205-211.

Dotto, T. S., Kerr, R., Mata, M. M., & Garcia, C. A. (2016). Multidecadal freshening and lightening in the deep waters of the Bransfield Strait, Antarctica. *Journal of Geophysical Research: Oceans, 121*, 3741-3756.

Downey, R. V., Griffiths, H. J., Linse, K., & Janussen, D. (2012). Diversity and distribution patterns in high southern latitude sponges. *PLoS One, 7*, e41672.

Dray, S., & Dufour, A. B. (2007). The ade4 package: implementing the duality diagram for ecologists. *Journal of Statistical Software, 22*, 1-20.

Ducklow, H. W., Fraser, W. R., Meredith, M. P., Stammerjohn, S. E., Doney, S. C., Martinson, D. G., ... & Amsler, C. D. (2013). West Antarctic Peninsula: an ice-dependent coastal marine ecosystem in transition. *Oceanography, 26*, 190-203.

Duran S., & Rützler K. (2006). Ecological speciation in a Caribbean marine sponge. *Molecular Phylogenetics and Evolution, 40*, 292–297.

Earl, D. A., & vonHoldt B. M. (2012). STRUCTURE HARVESTER: a website and program for visualizing STRUCTURE output and implementing the Evanno method. *Conservation Genetics Resources, 4*, 359-361.

Elderfield, H. (1972). Effects of volcanism on water chemistry, Deception Island, Antarctica. *Marine Geology, 13*, M1-M6.

Ereskovsky, A. V., & Tokina, D. B. (2004). Morphology and fine structure of the swimming

940 larvae of *Ircinia oros* (Porifera, Demospongiae, Dictyoceratida). *Invertebrate Reproduction &*
941 *Development, 45*, 137-150.
942
943 Ernster, L., & Schatz, G. (1981). Mitochondria: a historical review. *Journal of Cell Biology,*
944 *91*, 227s-255s.
945
946 Evanno, G., Regnaut, S., & Goudet, J. (2005). Detecting the number of clusters of individuals
947 using the software STRUCTURE: a simulation study. *Molecular Ecology, 14*, 2611-2620.
948
949 Fabriek, B. O., van Bruggen, R., Deng, D. M., Ligtenberg, A. J., Nazmi, K., Schornagel,
950 K., ... & van den Berg, T. K. (2009). The macrophage scavenger receptor CD163 functions as
951 an innate immune sensor for bacteria. *Blood, 113*, 887-892.
952
953 Ferchaud, A. L., & Hansen, M. M. (2016). The impact of selection, gene flow and
954 demographic history on heterogeneous genomic divergence: three□spine sticklebacks in
955 divergent environments. *Molecular Ecology, 25*, 238-259.
956
957 Filipowicz, W., Bhattacharyya, S. N., & Sonenberg, N. (2008). Mechanisms of post-
958 transcriptional regulation by microRNAs: are the answers in sight?. *Nature Reviews Genetics,*
959 *9*, 102.
960
961 Floris, M., Mahgoub, H., Lanet, E., Robaglia, C., & Menand, B. (2009). Post-transcriptional
962 regulation of gene expression in plants during abiotic stress. *International Journal of*
963 *Molecular Sciences, 10*, 3168-3185.
964
965 Foll, M., & Gaggiotti, O. (2008). A genome-scan method to identify selected loci appropriate
966 for both dominant and codominant markers: a Bayesian perspective. *Genetics, 180*, 977-993.
967
968 Galaska, M. P., Sands, C. J., Santos, S. R., Mahon, A. R., & Halanych, K. M. (2017a).
969 Geographic structure in the Southern Ocean circumpolar brittle star *Ophionotus victoriae*
970 (Ophiuridae) revealed from mtDNA and single□nucleotide polymorphism data. *Ecology and*
971 *Evolution, 7*, 475-485.
972
973 Galaska, M. P., Sands, C. J., Santos, S. R., Mahon, A. R., & Halanych, K. M. (2017b).
974 Crossing the divide: admixture across the Antarctic polar front revealed by the brittle star
975 *Astrotoma agassizii*. *The Biological Bulletin, 232*, 198-211.
976
977 Giles, E. C., Saenz□Agudelo, P., Hussey, N. E., Ravasi, T., & Berumen, M. L. (2015).
978 Exploring seascape genetics and kinship in the reef sponge *Stylissa carteri* in the Red Sea.
979 *Ecology and Evolution, 5*, 2487-2502.
980
981 Gleason, L. U., & Burton, R. S. (2016). Genomic evidence for ecological divergence against a
982 background of population homogeneity in the marine snail *Chlorostoma funebralis*.
983 *Molecular Ecology, 25*, 3557-3573.
984
985 González-Wevar, C. A., David, B., & Poulin, E. (2011). Phylogeography and demographic

inference in *Nacella* (Patinigera) concinna (Strebel, 1908) in the western Antarctic Peninsula. *Deep Sea Research Part II: Topical Studies in Oceanography, 58,* 220-229.

González-Wevar, C. A., Saucède, T., Morley, S. A., Chown, S. L., & Poulin, E. (2013). Extinction and recolonization of maritime A ntarctica in the limpet *Nacella concinna* (Strebel, 1908) during the last glacial cycle: toward a model of Quaternary biogeography in shallow A ntarctic invertebrates. *Molecular Ecology, 22*, 5221-5236.

Goudet, J. (2005). Hierfstat, a package for R to compute and test hierarchical F□statistics. *Molecular Ecology Notes, 5*, 184-186.

Grabherr, M. G., Haas, B. J., Yassour, M., Levin, J. Z., Thompson, D. A., Amit, I., ... & Chen, Z. (2011). Full-length transcriptome assembly from RNA-Seq data without a reference genome. *Nature Biotechnology, 29*, 644.

Halanych, K. M., & Mahon, A. R. (2018). Challenging dogma concerning biogeographic patterns of Antarctica and the Southern Ocean. *Annual Review of Ecology, Evolution, and Systematics, 49,* 355-378.

Hu, H., & Sun, S. C. (2016). Ubiquitin signaling in immune responses. *Cell Research, 26*, 457.

Huang, D., Meier, R., Todd, P. A., & Chou, L. M. (2008a). Slow mitochondrial COI sequence evolution at the base of the metazoan tree and its implications for DNA barcoding. *Journal of Molecular Evolution, 66*, 167-174.

Huang, D. W., Sherman, B. T., & Lempicki, R. A. (2008b). Systematic and integrative analysis of large gene lists using DAVID bioinformatics resources. *Nature Protocols, 4*, 44.

Huang, D. W., Sherman, B. T., & Lempicki, R. A. (2008c). Bioinformatics enrichment tools: paths toward the comprehensive functional analysis of large gene lists. *Nucleic Acids Research, 37*, 1-13.

Huneke, W. G. C., Huhn, O., & Schröeder, M. (2016). Water masses in the Bransfield Strait and adjacent seas, austral summer 2013. *Polar Biology, 39*, 789-798.

Intergovernmental Panel on Climate Change (IPCC). (2013). Climate Change 2013: The Physical Science Basis. Working Group I Contribution to the IPCC 5th Assessment Report—Changes to the Underlying Scientific/Technical Assessment.

Jacobs, A., Noia, M., Praebel, K., Kanstad-Hanssen, Ø., Paterno, M., Jackson, D., ... & Llewellyn, M. S. (2018). Genetic fingerprinting of salmon louse (*Lepeophtheirus salmonis*) populations in the North-East Atlantic using a random forest classification approach. *Scientific Reports, 8*, 1203.

Jakobsson, M., & Rosenberg, N. A. (2007). CLUMPP: a cluster matching and permutation

program for dealing with label switching and multimodality in analysis of population structure. *Bioinformatics, 23*, 1801-1806.

Jakoby, W. B., Bend, J. R., & Caldwell J. (2012). Metabolic Basis of Detoxification: Metabolism of Functional Groups. Ed Academic Press.

Janosik, A. M., Mahon, A. R., & Halanych, K. M. (2011). Evolutionary history of Southern Ocean *Odontaster* sea star species (Odontasteridae; Asteroidea). *Polar Biology, 34*, 575-586.

Jeffries, D. L., Copp, G. H., Lawson Handley, L., Olsén, K. H., Sayer, C. D., & Hänfling, B. (2016). Comparing RAD seq and microsatellites to infer complex phylogeographic patterns, an empirical perspective in the Crucian carp, *Carassius carassius*, L. *Molecular Ecology, 25*, 2997-3018.

Jin, Y. K., Lundgren, P., Lutz, A., Raina, J. B., Howells, E. J., Paley, A. S., ... & van Oppen, M. J. (2016). Genetic markers for antioxidant capacity in a reef-building coral. *Science Advances, 2*, e1500842.

Jombart, T. (2008). adegenet: a R package for the multivariate analysis of genetic markers. *Bioinformatics, 24*, 1403-1405.

Jombart, T., Devillard, S., & Balloux, F. (2010). Discriminant analysis of principal components: a new method for the analysis of genetically structured populations. *BMC Genetics, 11*, 94.

Jombart, T., & Ahmed, I. (2011). adegenet 1.3-1: new tools for the analysis of genome-wide SNP data. *Bioinformatics, 27*, 3070-3071.

Katoh, K., & Toh, H. (2008). Recent developments in the MAFFT multiple sequence alignment program. *Briefings in Bioinformatics, 9*, 286-298.

Katoh, K., & Standley, D. M. (2013). MAFFT multiple sequence alignment software version 7: improvements in performance and usability. *Molecular Biology and Evolution, 30*, 772-780.

Kearse, M., Moir, R., Wilson, A., Stones-Havas, S., Cheung, M., Sturrock, S., ... & Thierer, T. (2012). Geneious Basic: an integrated and extendable desktop software platform for the organization and analysis of sequence data. *Bioinformatics, 28*, 1647-1649.

Kedersha, N., & Anderson, P. (2002). Stress granules: sites of mRNA triage that regulate mRNA stability and translatability. *Biochemical Society Transactions, 30*, 963-969.

Kedersha, N., Chen, S., Gilks, N., Li, W., Miller, I. J., Stahl, J., & Anderson, P. (2002). Evidence that ternary complex (eIF2-GTP-tRNAi Met)–deficient preinitiation complexes are core constituents of mammalian stress granules. *Molecular Biology of the Cell, 13*, 195-210.

Keenan, K., McGinnity, P., Cross, T. F., Crozier, W. W., & Prodöhl, P. A. (2013). diveRsity: an R package for the estimation and exploration of population genetics parameters and their associated errors. *Methods in Ecology and Evolution, 4*, 782-788.

Kendall, M. S., Poti, M., Wynne, T. T., Kinlan, B. P., & Bauer, L. B. (2013). Consequences of the life history traits of pelagic larvae on interisland connectivity during a changing climate. *Marine Ecology Progress Series, 489*, 43-59.

King, J. C. (1994). Recent climate variability in the vicinity of the Antarctic Peninsula. *International Journal of Climatology, 14*, 357-369.

King, J. C., & Harangozo, S. A. (1998). Climate change in the western Antarctic Peninsula since 1945: observations and possible causes. *Annals of Glaciology, 27,* 571-575.

Koutsouveli, V., Taboada, S., Moles, J., Cristobo, J., Ríos, P., Bertran, A., ... & Riesgo, A. (2018). Insights into the reproduction of some Antarctic dendroceratid, poecilosclerid, and haplosclerid demosponges. *PloS one, 13*, e0192267.

Krabbe, K., Leese, F., Mayer, C., Tollrian, R., & Held, C. (2010). Cryptic mitochondrial lineages in the widespread pycnogonid *Colossendeis megalonyx* Hoek, 1881 from Antarctic and Subantarctic waters. *Polar Biology, 33*, 281-292.

Kültz, D. (2003). Evolution of the cellular stress proteome: from monophyletic origin to ubiquitous function. *Journal of Experimental Biology, 206*, 3119-3124.

Kwon, S., Zhang, Y., & Matthias, P. (2007). The deacetylase HDAC6 is a novel critical component of stress granules involved in the stress response. *Genes & Development, 21*, 3381-3394.

Leiva, C., Riesgo, A., Avila, C., Rouse, G. W., & Taboada, S. (2018). Population structure and phylogenetic relationships of a new shallow□water Antarctic phyllodocid annelid. *Zoologica Scripta, 47*, 714-726.

León-Pech, M. G., Cruz-Barraza, J. A., Carballo, J. L., Calderon-Aguilera, L. E., & Rocha-Olivares, A. (2015). Pervasive genetic structure at different geographic scales in the coral-excavating sponge *Cliona vermifera* (Hancock, 1867) in the Mexican Pacific. *Coral Reefs, 34*, 887-897.

Li, B., & Dewey, C. N. (2011). RSEM: accurate transcript quantification from RNA-Seq data with or without a reference genome. *BMC Bioinformatics, 12*, 323.

Librado, P., & Rozas, J. (2009). DnaSP v5: a software for comprehensive analysis of DNA polymorphism data. *Bioinformatics, 25*, 1451-1452.

Limborg, M. T., Helyar, S. J., De Bruyn, M., Taylor, M. I., Nielsen, E. E., Ogden, R. O. B., ... & Bekkevold, D. (2012). Environmental selection on transcriptome-derived SNPs in a high

gene flow marine fish, the Atlantic herring (*Clupea harengus*). *Molecular Ecology, 21*, 3686-3703.

López-Legentil, S., & Pawlik, J. R. (2009) Genetic structure of the Caribbean giant barrel sponge *Xestospongia muta* using the I3-M11 partition of COI. *Coral Reefs, 28*, 157-165.

Loschi, M., Leishman, C. C., Berardone, N., & Boccaccio, G. L. (2009). Dynein and kinesin regulate stress-granule and P-body dynamics. *Journal of Cell Science, 122*, 3973-3982.

Luria, C. M., Ducklow, H. W., & Amaral-Zettler, L. A. (2014). Marine bacterial, archaeal and eukaryotic diversity and community structure on the continental shelf of the western Antarctic Peninsula. *Aquatic Microbial Ecology, 73*, 107-121.

Maldonado, M. (2006). The ecology of the sponge larva. *Canadian Journal of Zoology, 84*, 175-194.

Manni, F., Guerard, E., & Heyer, E. (2004). Geographic patterns of (genetic, morphologic, linguistic) variation: how barriers can be detected by using Monmonier's algorithm. *Human Biology, 76*, 173-190.

McKenzie, C. W., Craige, B., Kroeger, T. V., Finn, R., Wyatt, T. A., Sisson, J. H., ... & Lee, L. (2015). CFAP54 is required for proper ciliary motility and assembly of the central pair apparatus in mice. *Molecular Biology of the Cell, 26*, 3140-3149.

McKinney, G. J., Larson, W. A., Seeb, L. W., & Seeb, J. E. (2017). RAD seq provides unprecedented insights into molecular ecology and evolutionary genetics: comment on Breaking RAD by Lowry et al.(2016). *Molecular Ecology Resources, 17*, 356-361.

Meijers, A. J. S. (2014). The Southern Ocean in the coupled model intercomparison project phase 5. *Philosophical Transactions of the Royal Society A: Mathematical, Physical and Engineering Sciences, 372*, 20130296.

Meredith, M. P., & King, J. C. (2005). Rapid climate change in the ocean west of the Antarctic Peninsula during the second half of the 20th century. *Geophysical Research Letters, 32*, L19604.

Moffat, C., Beardsley, R. C., Owens, B., & Van Lipzig, N. (2008). A first description of the Antarctic Peninsula Coastal Current. *Deep Sea Research Part II: Topical Studies in Oceanography, 55*, 277-293.

Moles, J., Wägele, H., Cutignano, A., Fontana, A., Ballesteros, M., & Avila, C. (2017). Giant embryos and hatchlings of Antarctic nudibranchs (Mollusca: Gastropoda: Heterobranchia). *Marine Biology, 164*, 114.

Morán, X. A. G., Gasol, J. M., Pedrós-Alió, C., & Estrada, M. (2001). Dissolved and particulate primary production and bacterial production in offshore Antarctic waters during

austral summer: coupled or uncoupled? *Marine Ecology Progress Series, 222*, 25-39.

Morán, X. A. G., & Estrada, M. (2002). Phytoplanktonic DOC and POC production in the Bransfield and Gerlache Straits as derived from kinetic experiments of 14C incorporation. *Deep Sea Research Part II: Topical Studies in Oceanography, 49*, 769-786.

Narum, S. R., & Hess, J. E. (2011). Comparison of F_{ST} outlier tests for SNP loci under selection. *Molecular Ecology Resources, 11*, 184-194.

Nei, M. (1973). Analysis of gene diversity in subdivided populations. *Proceedings of the National Academy of Sciences of the USA, 70*, 3321-3323.

O'Connor, M. I., Bruno, J. F., Gaines, S. D., Halpern, B. S., Lester, S. E., Kinlan, B. P., & Weiss, J. M. (2007). Temperature control of larval dispersal and the implications for marine ecology, evolution, and conservation. *Proceedings of the National Academy of Sciences of the USA, 104*, 1266-1271.

Ortiz, R., Vila, J., García, A., Camacho, A. G., Diez, J. L., Aparicio, A., ... & Petrinovic, I. (1992). Geophysical features of Deception Island. *Recent Progress in Antarctic Earth Science,* 443-448.

Paradis, E. (2010). pegas: an R package for population genetics with an integrated–modular approach. *Bioinformatics, 26*, 419-420.

Pascual, M., Rives, B., Schunter, C., & Macpherson, E. (2017). Impact of life history traits on gene flow: a multispecies systematic review across oceanographic barriers in the Mediterranean Sea. *PLoS One, 12*, e0176419.

Paradis, E., Claude, J., & Strimmer, K. (2004). APE: analyses of phylogenetics and evolution in R language. *Bioinformatics, 20*, 289-290.

Pazmiño, D. A., Maes, G. E., Simpfendorfer, C. A., Salinas-de-León, P., & van Herwerden, L. (2017). Genome-wide SNPs reveal low effective population size within confined management units of the highly vagile Galapagos shark (*Carcharhinus galapagensis*). *Conservation Genetics, 18*, 1151-1163.

Peck, L. S., & Conway, L. Z. (2000). The myth of metabolic cold adaptation: oxygen consumption in stenothermal Antarctic bivalves. *Geological Society, London, Special Publications, 177*, 441-450.

Peck, L. S., Webb, K. E., & Bailey, D. M. (2004). Extreme sensitivity of biological function to temperature in Antarctic marine species. *Functional Ecology, 18*, 625-630.

Pérez-Portela, R., Noyer, C., & Becerro, M. A. (2015). Genetic structure and diversity of the endangered bath sponge *Spongia lamella*. *Aquatic Conservation: Marine and Freshwater Ecosystems, 25*, 365-379.

Pérez-Portela, R., & Riesgo, A. (2018). Population Genomics of Early-Splitting Lineages of Metazoans. In: Population Genomics. 1-35. Springer, Cham.

Peterson, B. K., Weber, J. N., Kay, E. H., Fisher, H. S., & Hoekstra, H. E. (2012). Double digest RADseq: an inexpensive method for de novo SNP discovery and genotyping in model and non-model species. *PloS one, 7*, e37135.

Pita, L., Hoeppner, M. P., Ribes, M., & Hentschel, U. (2018). Differential expression of immune receptors in two marine sponges upon exposure to microbial-associated molecular patterns. *Scientific Reports, 8*, 16081.

Plese, B., Rossi, M. E., Kenny, N., Taboada, S., Koutsouveli, V., & Riesgo, A. (2018). Trimitomics: An efficient pipeline for mitochondrial assembly from transcriptomic reads in non-model species. *bioRxiv*, 413138.

Pritchard, J. K., Stephens, M., & Donnelly, P. (2000). Inference of population structure using multilocus genotype data. *Genetics, 155*, 945-959.

R Core Team (2014). A language and environment for statistical computing. http://www.R-project.org.

Reitzel, A. M., Herrera, S., Layden, M. J., Martindale, M. Q., & Shank, T. M. (2013). Going where traditional markers have not gone before: utility of and promise for RAD sequencing in marine invertebrate phylogeography and population genomics. *Molecular Ecology, 22*, 2953-2970.

Riesgo, A., Taboada, S., & Avila, C. (2015). Evolutionary patterns in Antarctic marine invertebrates: An update on molecular studies. *Marine Genomics, 23*, 1-13.

Riesgo, A., Pérez-Portela, R., Pita, L., Blasco, G., Erwin, P. M., & López-Legentil, S. (2016). Population structure and connectivity in the Mediterranean sponge *Ircinia fasciculata* are affected by mass mortalities and hybridization. *Heredity, 117*, 427.

Rogers, A. D. (2007). Evolution and biodiversity of Antarctic organisms: a molecular perspective. *Philosophical Transactions of the Royal Society of London B: Biological Sciences, 362*, 2191-2214.

Sanford, E., & Kelly, M. W. (2011). Local adaptation in marine invertebrates. *Annual Review of Marine Science, 3,* 509-535.

Sangrà, P., Gordo, C., Hernández-Arencibia, M., Marrero-Díaz, A., Rodríguez-Santana, A., Stegner, A., ... & Pichon, T. (2011). The Bransfield current system. *Deep Sea Research Part I: Oceanographic Research Papers, 58*, 390-402.

Sarà, M., Balduzzi, A., Barbieri, M., Bavestrello, G., & Burlando, B. (1992). Biogeographic

traits and checklist of Antarctic demosponges. *Polar Biology, 12*, 559-585.

Setiawan, E., de Voogd, N. J., Swierts, T., Hooper, J. N., Wörheide, G., & Erpenbeck, D. (2016). MtDNA diversity of the Indonesian giant barrel sponge *Xestospongia testudinaria* (Porifera: Haplosclerida)–implications from partial cytochrome oxidase 1 sequences. *Journal of the Marine Biological Association of the United Kingdom, 96*, 323-332.

Stammerjohn, S. E., Martinson, D. G., Smith, R. C., & Iannuzzi, R. A. (2008). Sea ice in the western Antarctic Peninsula region: Spatio-temporal variability from ecological and climate change perspectives. *Deep Sea Research Part II: Topical Studies in Oceanography, 55*, 2041-2058.

Sugg, D. W., Chesser, R. K., Dobson, F. S., & Hoogland, J. L. (1996). Population genetics meets behavioral ecology. *Trends in Ecology & Evolution, 11*, 338-342.

Taboada, S., Riesgo, A., Wiklund, H., Paterson, G. L., Koutsouveli, V., Santodomingo, N., ... & Glover, A. G. (2018). Implications of population connectivity studies for the design of marine protected areas in the deep sea: An example of a demosponge from the Clarion□ Clipperton Zone. *Molecular Ecology, 27,* 4657-4679.

Tajima, F. (1989). Statistical method for testing the neutral mutation hypothesis by DNA polymorphism. *Genetics, 123*, 585-595.

Takahashi, M., Higuchi, M., Matsuki, H., Yoshita, M., Ohsawa, T., Oie, M., & Fujii, M. (2013). Stress granules inhibit apoptosis by reducing reactive oxygen species production. *Molecular and Cellular Biology, 33*, 815-829.

Thatje, S., Hillenbrand, C. D., & Larter, R. (2005). On the origin of Antarctic marine benthic community structure. *Trends in Ecology & Evolution, 20*, 534-540.

Thornhill, D. J., Mahon, A. R., Norenburg, J. L., & Halanych, K. M. (2008). Open□ocean barriers to dispersal: a test case with the Antarctic Polar Front and the ribbon worm *Parborlasia corrugatus* (Nemertea: Lineidae). *Molecular Ecology, 17*, 5104-5117.

Tigano, A., Shultz, A. J., Edwards, S. V., Robertson, G. J., & Friesen, V. L. (2017). Outlier analyses to test for local adaptation to breeding grounds in a migratory arctic seabird. *Ecology and Evolution, 7*, 2370-2381.

Turner, J., Colwell, S. R., Marshall, G. J., Lachlan□Cope, T. A., Carleton, A. M., Jones, P. D., ... & Iagovkina, S. (2005). Antarctic climate change during the last 50 years. *International Journal of Climatology, 25*, 279-294.

van Oppen, M. J., Bongaerts, P., Frade, P., Peplow, L. M., Boyd, S. E., Nim, H. T., & Bay, L. K. (2018). Adaptation to reef habitats through selection on the coral animal and its associated microbiome. *Molecular Ecology, 27*, 2956-2971.

1308 Vaughan, D. G., Marshall, G. J., Connolley, W. M., Parkinson, C., Mulvaney, R., Hodgson,
1309 D. A., ... & Turner, J. (2003). Recent rapid regional climate warming on the Antarctic
1310 Peninsula. *Climatic Change, 60*, 243-274.
1311
1312 Vernet, M., Martinson, D., Iannuzzi, R., Stammerjohn, S., Kozlowski, W., Sines, K., ... &
1313 Garibotti, I. (2008). Primary production within the sea-ice zone west of the Antarctic
1314 Peninsula: I—Sea ice, summer mixed layer, and irradiance. *Deep Sea Research Part II:*
1315 *Topical Studies in Oceanography, 55*, 2068-2085.
1316
1317 Vicente-Manzanares, M., & Sánchez-Madrid, F. (2004). Role of the cytoskeleton during
1318 leukocyte responses. *Nature Reviews Immunology, 4*, 110.
1319
1320 Wickramarachchi, D. C., Theofilopoulos, A. N., & Kono, D. H. (2010). Immune pathology
1321 associated with altered actin cytoskeleton regulation. *Autoimmunity, 43*, 64-75.
1322
1323 Wiens, M., Korzhev, M., Perović-Ottstadt, S., Luthringer, B., Brandt, D., Klein, S., & Müller,
1324 W. E. (2006). Toll-like receptors are part of the innate immune defense system of sponges
1325 (Demospongiae: Porifera). *Molecular Biology and Evolution, 24*, 792-804.
1326
1327 Xavier, J. R., Rachello-Dolmen, P. G., Parra-Velandia, F., Schönberg, C. H. L., Breeuwer, J.
1328 A. J., & Van Soest, R. W. M. (2010). Molecular evidence of cryptic speciation in the
1329 "cosmopolitan" excavating sponge *Cliona celata* (Porifera, Clionaidae). *Molecular*
1330 *Phylogenetics and Evolution, 56*, 13-20.
1331
1332 Zerbino, D., & Birney, E. (2008). Velvet: algorithms for de novo short read assembly using de
1333 Bruijn graphs. *Genome Research, 18*, 821-829, gr-074492.
1334
1335 Zhou, M., Niiler, P. P., & Hu, J. H. (2002). Surface currents in the Bransfield and Gerlache
1336 straits, Antarctica. *Deep Sea Research Part I: Oceanographic Research Papers, 49*, 267-280.
1337
1338 Zhou, M., Niiler, P. P., Zhu, Y., & Dorland, R. D. (2006). The western boundary current in
1339 the Bransfield Strait, Antarctica. *Deep Sea Research Part I: Oceanographic Research Papers,*
1340 *53*, 1244-1252.

DATA ACCESSIBILITY

RAD-seq data for each individual sample are deposited in the NCBI SRA database, BioProject PRJNA531366, Biosamples SAMN11350306 - SAMN11350367. Data of the three transcriptomes are deposited in the same BioProject under accession numbers SRR8886798, SRR8886808, and SRR8886813. Alignments of the 15 mitochondrial genes and vcf files of both the neutral dataset and the SNPs under positive selection are found in Supplementary Material 1-3.

AUTHOR CONTRIBUTIONS

C.L., S.T., G.G., and A.R. conceived and designed the study; C.L. and G.G. conducted fieldwork and collected samples; C.L., S.T., D.C. and N.J.K. conducted laboratory work; C.L., S.T., T.J., N.J.K., and A.R. performed statistical analyses and interpreted the results; C.L., S.T., and A.R. wrote the manuscript, and all authors edited various versions of the manuscript.

Figure Legends

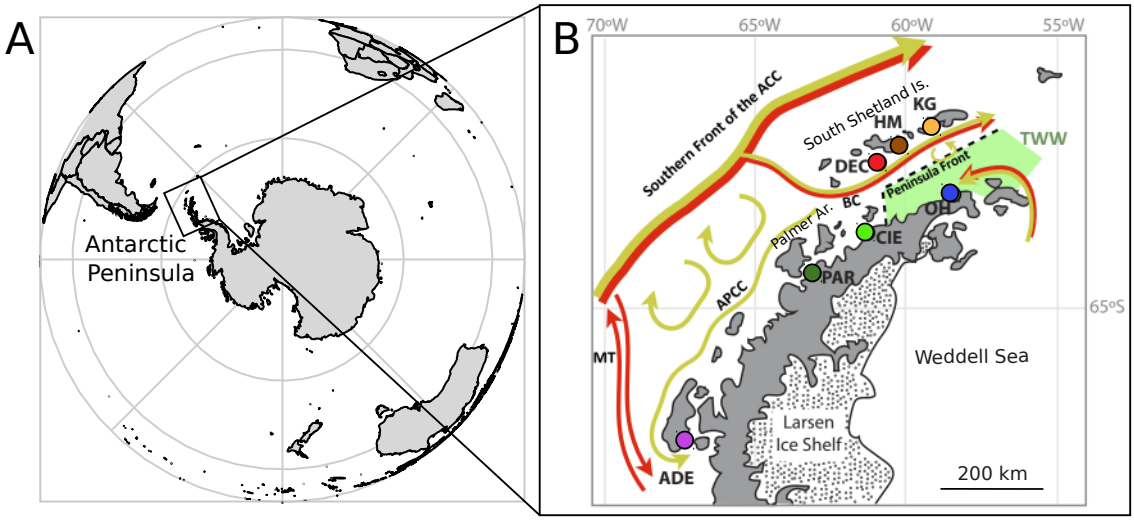

FIGURE 1 (A) Map of Antarctica showing the study area. (B) Detailed map of the Antarctic Peninsula, South Shetland archipelago and adjacent islands, showing sampling sites: KG, King George Island; HM, Half Moon Island; DEC, Deception Island; OH, O'Higgins Bay; CIE, Cierva Cove; PAR, Paradise Bay; ADE, Adelaide Island. Oceanic currents and water masses of the study area are outlined. Yellow and red arrows represent surface and deep currents, respectively; green shadowed area on the tip of the WAP correspond to the Transitional Water with Weddell Sea Influence (TWW), delimited by the Peninsula Front represented by a black dashed line. APCC, Antarctic Peninsula Coastal Current; MT, Marguerite Trough CDW Intrusion; BC, Bransfield Current.

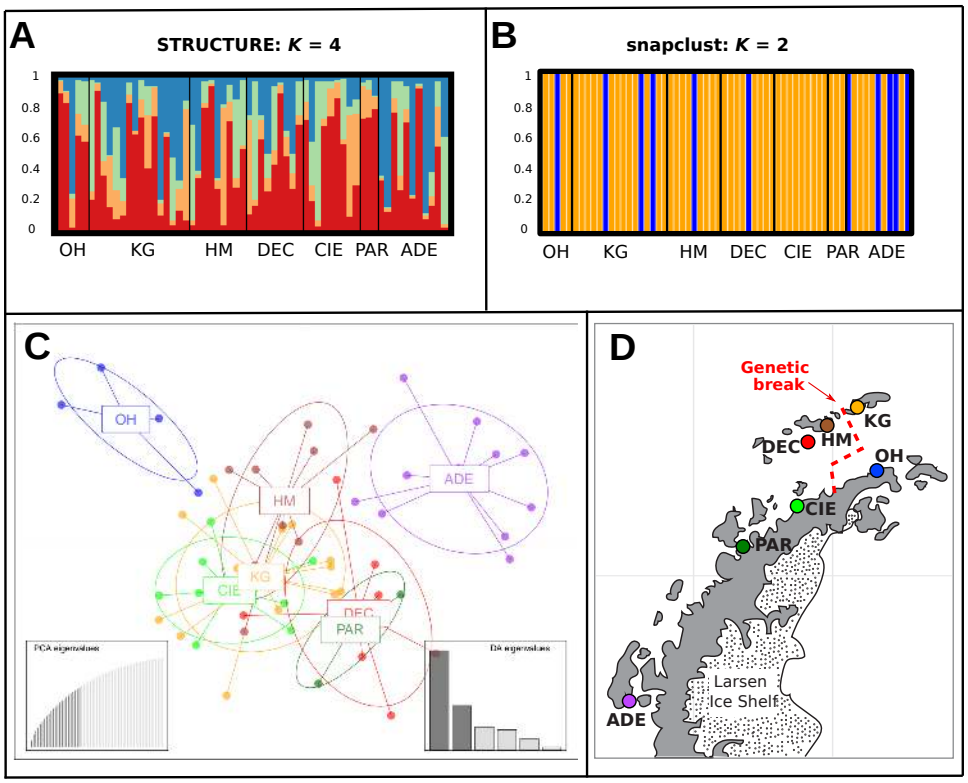

FIGURE 2 Population structure and differentiation analyses based on the 389 neutral SNPs dataset. (A) STRUCTURE results with $K = 4$ (see delta K plot at Supplementary Material 4), (B) *snapclust* results with $K = 2$ (see AIC plot at Supplementrary Material 4), (C) DAPC results: two-dimension representation of the first (horizontal axis) and second (vertical axis) PCA eigenvalues. (D) Map of the study area with the genetic break from the Barrier analysis showed as a red dashed line. See abbreviations in Figure 1.

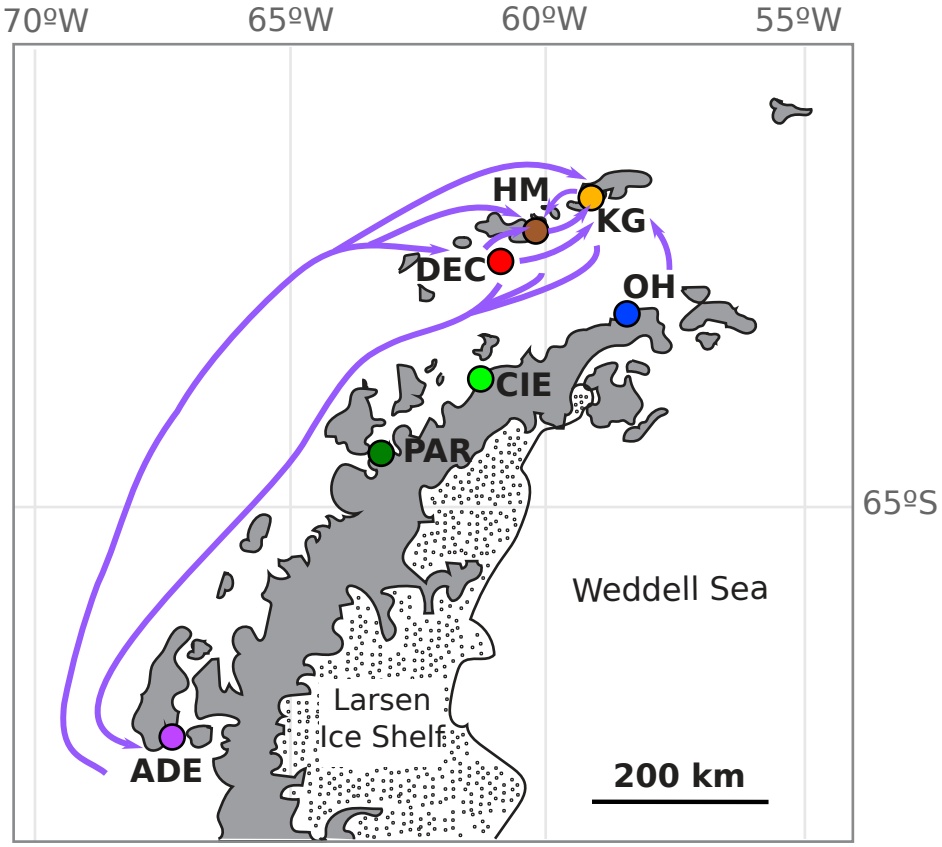

FIGURE 3 Contemporary migration network inferred from *divMigrate*. Map of the study area with purple arrows representing the migration values higher than 0.8 in the migration table (see Supplementary Material 7).

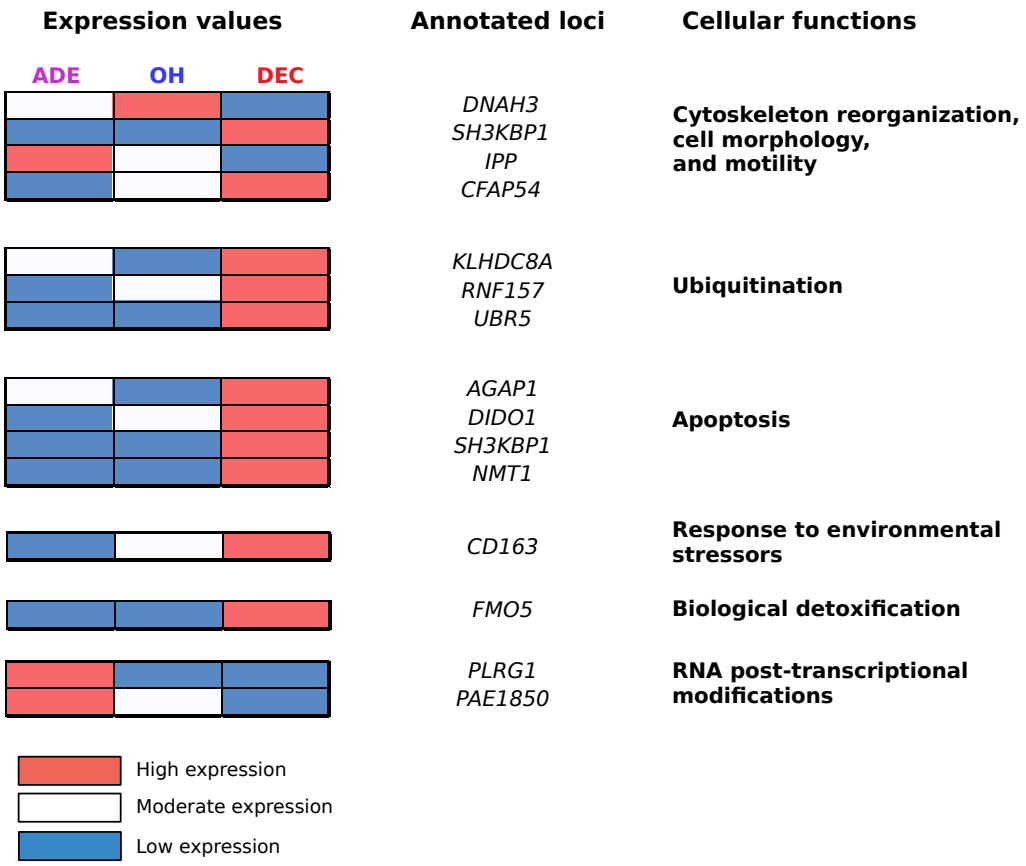

FIGURE 4 Functional annotation analysis showing the 14 annotated loci under selection, their cellular function, and relative expression levels presented in heatmaps (actual values can be seen in Table 5). Red indicates higher expression, white moderate expression, and blue low expression, based on the values reported in Table 5.

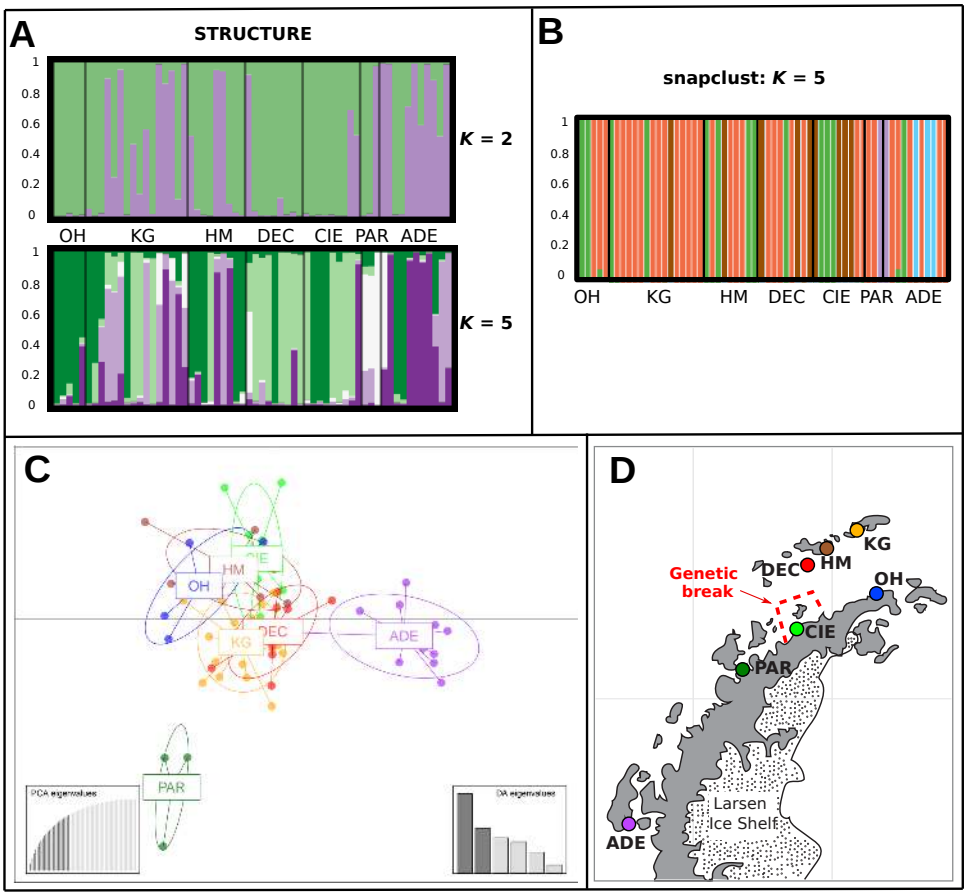

FIGURE 5 Genetic structure results based on the 140 outlier SNPs under positive selection. (A) STRUCTURE results with $K = 2$ and $K = 5$, first and second most probable number of clusters, respectively (see delta K plot at Supplementary Material 4), (B) *snapclust* results with $K = 5$ (see AIC plot at Supplementrary Material 4), (C) DAPC results: two-dimension representation of the first (horizontal axis) and second (vertical axis) PCA eigenvalues. (D) Map of the study area with the genetic break from the Barrier analysis showed as a red dashed line. See abbreviations in Figure 1.

Table legends

Station	Abbreviation	Coordinates	Number of individuals	Date of collection
Deception Island	DEC	62º59'25"S 60º37'31"W	9	13/1/2016
Half Moon Island	HM	62º35'41"S 59º54'07"W	9	24/2/2016
King George Island	KG	62º11'55"S 58º56'59"W	16	21/2/2016
O'Higgins Bay	OH	63º18'52"S 57º54'27"W	5	19/2/2016
Cierva Cove	CIE	64º09'20"S 60º57'12"W	9	17/2/2016
Paradise Bay	PAR	64º49'24"S 62º51'24"W	3	15/2/2016
Adelaide Island	ADE	67º34'04"S 68º08'55"W	11	12/2/2016
TOTAL			62	

Table 1. Collection details for all sampling sites, including abbreviations, coordinates, number of individuals used in the analyses, and date of collection.

	D	Av *He*	Av *Ho*	*He* – *Ho*	H-W	*Fis*
Cierva Cove	**-4.180**	0.126	0.075	0.051	5/385	0.405
Deception Is.	**-4.182**	0.131	0.076	0.055	4/388	0.420
Half Moon Is.	**-4.227**	0.133	0.079	0.054	7/389	0.406
King George Is.	**-3.830**	0.142	0.062	0.080	27/388	0.563
O'Higgins Bay	**-3.881**	0.121	0.062	0.059	1/387	0.488
Paradise Bay	**-3.634**	0.054	0.052	0.002	0/319	0.037
Adelaide Is.	**-4.069**	0.138	0.053	0.085	22/389	0.616
TOTAL	**-3.321**	0.162	0.067	0.095	178/389	0.586

Table 2. Population genetic statistics and demographic estimators from the 389 neutral SNPs dataset. *D*, Tajima's *D* values, bold numbers showing significant deviation from 0; Av *He*, averaged expected heterozygosity; Av *Ho*, averaged observed heterozygosity; *He* - *Ho*, difference between averaged expected and averaged observed heterozygosities; H-W, number of SNPs not in Hardy-Weinberg equilibrium compared to the total SNPs obtained for each station; F_{IS}, inbreeding coefficient estimated from averaged observed and averaged expected heterozygosities.

	Cierva Cove	Deception Is.	King George Is.	Half Moon Is.	O'Higgins Bay	Paradise Bay	Adelaide Is.
Cierva Cove		0.102	0.077	0.114	0.119	0	0.121
Deception Is.	**0.302**		0.073	0.102	0.123	0	0.106
King George Is.	**0.210**	0.141		0.084	0.073	0	0.094
Half Moon Is.	**0.208**	**0.238**	0.121		0.124	0	0.094
O'Higgins Bay	**0.421**	**0.280**	**0.150**	**0.167**		0	0.102
Paradise Bay	**0.204**	0.063	0.099	0.167	0.017		0
Adelaide Is.	**0.323**	**0.301**	**0.220**	**0.231**	**0.250**	0.120	

Table 3. Pairwise F_{ST} values for the neutral SNP dataset (above diagonal) and the dataset composed of putative SNPs under positive selection (below diagonal). Significant F_{ST} values (p-value < 0.05) are shown in bold.

	Df	Sum Sq	Mean Sq	Percentage of variation	p-value
A) Neutral Dataset					
DAPC: ADE / OH / Rest					
Between DAPC clusters	2	296.97	148.48	-0.15	0.468
Between populations	4	610.61	152.65	0.78	0.283
Between samples	55	7731.82	140.58	59.21	**0.001**
Within samples	62	2207.68	35.61	40.17	**0.001**
Barrier: KG + OH / Rest					
Between Barrier clusters	1	178.45	178.45	0.61	0.248
Between populations	5	729.13	145.83	0.37	0.373
Between samples	55	7731.82	140.58	59	**0.001**
Within samples	62	2207.68	35.61	40.02	**0.001**
B) Positive Selection Dataset					
DAPC: ADE / PAR / Rest					
Between DAPC clusters	2	291.76	145.88	6.72	**0.043**
Between populations	4	370.48	92.62	4.03	**0.002**
Between samples	55	3482.35	63.32	72.38	**0.001**
Within samples	62	409.65	6.61	16.87	**0.001**
Barrier: CIE / Rest					
Between Barrier clusters	1	128.11	128.11	1.45	0.124
Between populations	5	534.13	106.83	6.77	**0.001**
Between samples	55	3482.35	63.32	74.43	**0.001**
Within samples	62	409.45	6.61	17.35	**0.001**

Table 4. Hierarchical AMOVA results. Evaluation of genetic differentiation within and among sampling stations, and within and among the groups inferred from the DAPC and Barrier results for the 389 neutral SNPs dataset (A) and the 140 under positive selection SNPs dataset (B).

RAD-tag	Contig in reference transcriptome	Annotation	Abbreviation	E-value
3332	TRINITY_DN40585_c0_g1_i1	dimethylaniline monooxygenase [N-oxide-forming] 5	FMO5	1.87E-20
7288	TRINITY_DN35887_c1_g1_i1	actin-binding protein IPP-like	IPP	6.05E-42
9345	TRINITY_DN29758_c0_g1_i1	arf-GAP with GTPase, ANK repeat and PH domain-containing protein 1-like	AGAP1	7.54E-23
11872	TRINITY_DN30313_c0_g1_i1	cilia and flagella associated protein 54	CFAP54	5.13E-64
9419	TRINITY_DN36218_c2_g3_i4	death-inducer obliterator 1-like	DIDO1	1.29E-27
390	TRINITY_DN46058_c0_g1_i1	dynein heavy chain 3	DNAH3	6.37E-08
14033	TRINITY_DN17138_c0_g1_i1	E3 ubiquitin-protein ligase UBR5	UBR5	4.64E-12
9205	TRINITY_DN31666_c0_g1_i3	glycylpeptide N-tetradecanoyltransferase 1	NMT1	5.13E-64
1845	TRINITY_DN36199_c4_g2_i2	kelch domain-containing protein 8A	KLHDC8A	1.12E-52
2166	TRINITY_DN36199_c4_g2_i4	kelch domain-containing protein 8A	KLHDC8A	6.46E-45
7585	TRINITY_DN42392_c0_g1_i1	pleiotropic regulator 1-like	PLRG1	2.27E-29
2069	TRINITY_DN17268_c1_g1_i1	putative scavenger receptor cysteine-rich protein type 12 isoform X1	CD163L1	2.35E-38
2347	TRINITY_DN27486_c0_g1_i1	RING finger protein 157	RNF157	5.13E-64
3110	TRINITY_DN27486_c0_g1_i1	RING finger protein 157	RNF157	2.01E-63
6870	TRINITY_DN36204_c5_g4_i24	RRNA intron-encoded homing endonuclease	PAE1850	1.92E-60
4535	TRINITY_DN34338_c2_g1_i2	SH3 domain-containing kinase-binding protein 1-like isoform X2	SH3KBP1	2.71E-13
2011	TRINITY_DN46934_c0_g1_i1	uncharacterised protein	----	1.25E-61
9873	TRINITY_DN25724_c0_g1_i1	aminotransferase BACTERIA	----	5.13E-64

Table 5. Genes (and their corresponding RAD-tags) under positive selection in *Dendrilla antarctica,* alongside BLAST annotations and expression values in the three transcriptome samples.

Supplementary Material legends

SUPPLEMENTARY MATERIAL 1 vcf file of the neutral dataset (389 SNPs, 62 individuals).

SUPPLEMENTARY MATERIAL 2 vcf file of the SNPs under positive selection (140 SNPs, 62 individuals).

SUPPLEMENTARY MATERIAL 3 Alignments of the 15 mitochondrial genes, recovered from the draft-level genomic sequencing of an individual from Deception Island (gen_DEC), and from the transcriptomes of three individuals from Adelaide Island (Den_ADE_3_1500), Deception Island (Den_DEC_19_706), and O'Higgins Bay (Den_OH_2_2675).

SUPPLEMENTARY MATERIAL 4 Delta *K* and AIC plots for STRUCTURE and *snapclust* analyses, respectively, showing the most probable number of clusters for the 389 neutral SNPs dataset (A and B) and for the 140 under positive selection SNPs dataset (C and D).

SUPPLEMENTARY MATERIAL 5 (A) STRUCTURE results for the dataset just including the 210 neutral SNPs in Hardy-Weinberg equilibrium. (B) Delta *K* plot showing 2 clusters as the most likely number of clusters.

SUPPLEMENTARY MATERIAL 6 Two-dimensional representation of the DAPC results taking the first and third DAPC axes for the (A) neutral dataset and the (B) 140 SNPs under positive selection.

SUPPLEMENTARY MATERIAL 7 Pairwise G_{ST} migration table composed of two triangular matrices showing the estimated relative contemporary migration values for each pair of stations. Each value in the matrix, a_{ij}, represents the migration flow from station i to station j with a relative *a* intensity from 0 to 1.